High-Affinity Alkynyl Bisubstrate Inhibitors of NicotinamideN-Methyltransferase (NNMT)

High-Affinity Alkynyl Bisubstrate Inhibitors of Nicotinamide N-Methyltransferase (NNMT)

SUPPORTING INFORMATION PART 3

Rocco L. Policarpo[a], Ludovic Decultot[a], Elizabeth May[b], Petr Kuzmič[c], Sam Carlson[b], Danny Huang[a], Vincent Chu[a,1], Brandon Wright[b,2], Saravanakumar Dhakshinamoorthy[d], Aimo Kannt[e], Shilpa Rani[d], Sreekanth Dittakavi[d], Joseph Panarese[a,3], Rachelle Gaudet[b], Matthew D. Shair[*,a]

[a]*Department of Chemistry and Chemical Biology, Harvard University, Cambridge MA 02138, USA*
[b]*Department of Molecular and Cellular Biology, Harvard University, Cambridge MA 02138, USA*
[c]*BioKin Ltd., Watertown, Massachusetts*
[d]*Jubilant Biosys Ltd., Yeshwantpur Bangalore - 560 022, Karnataka, India*
[e]*Sanofi Research and Development, Industriepark Hoechst, H823, D-65926, Frankfurt am Main, Germany*

Abstract

This *Supporting Information* document contains a detailed description of all enzyme-kinetics analyses performed in order to characterize the 35 NNMT inhibitors listed in the main manuscript. In addition, we document detailed substrate-kinetic properties of NNMT under the conditions of the inhibitor screening assay. In particular, the fluorescence signal generated in the NNMT assay is strongly nonlinear due to two separate factors, namely, product inhibition and partial enzyme deactivation. Partial NNMT deactivation appears to proceed by a first-order decay of the Michaelis complex.

Key words:
nicotinamide N-methyltransferase; inhibition; bisubstrate analogs; molecular mechanism; kinetics; slow-binding; tight-binding

Contents

*Corresponding author
[1]Current address: Department of Cell Biology, Harvard Medical School, 240 Longwood Ave., Boston, MA 02115, USA
[2]Current address: Department of Chemistry, University of California, Berkeley, CA 94720, USA
[3]Current address: Enanta Pharmaceuticals, 500 Arsenal St., Watertown, MA 02472, USA

1. Substrate kinetic properties of SAM

In this section we describe the data-analytic procedure that was used to establish the basic kinetic properties of the substrate SAM, which were subsequently used as fixed model parameters in the analysis of the inhibition data.

1.1. Raw experimental data

The raw experimental data are shown in *Figure S1*. Three replicated experiments were performed and analyzed; two of the three replicates are shown. The reaction progress curves (fluorescence changes over time) were strongly nonlinear, which necessitated a choice of an appropriate nonlinear fitting model.

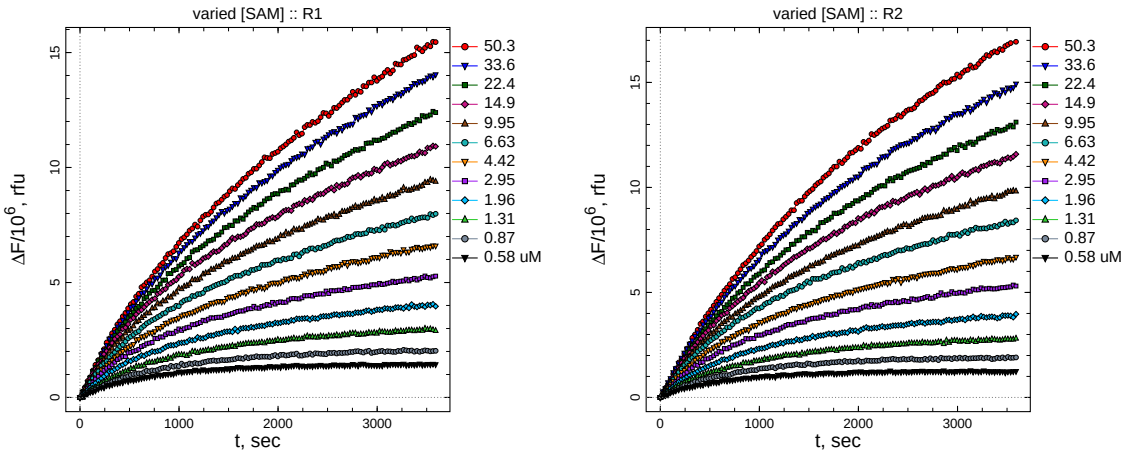

Replicate 1/3 Replicate 2/3

Figure S1: Raw experimental data from assays of NNMT conducted at 100 μM quinoline and 33 nM enzyme.

1.2. Theoretical models

In order to fully explain the strong nonlinearity of the reaction progress curves, as illustrated in *Figure S1*, we have devised two sets of mechanistic models. In a preliminary round of kinetic analysis (results not shown) we hypothesized that the nonlinear reaction time course could be caused by any possible combination of the following factors:

1. substrate depletion;
2. product inhibition;
3. enzyme deactivation caused by the free enzyme E decaying via a first-order process;
4. enzyme deactivation caused by the Michaelis complex E.S decaying via a first-order process.
5. enzyme deactivation caused by both the free enzyme E and the Michaelis complex E.S decaying via a first-order processes.

The choice of multiple possible pathways for enzyme deactivation was informed by our previously published results [1]; see also [2] for a more detailed discussion. In this preliminary round of model discrimination analysis, we were able to unambiguously exclude the possibility that the free enzyme E undergoes deactivation. However, denaturation of the Michaelis complex E.S could not be excluded. In a follow-up refinement analysis we therefore set up a model discrimination analysis using four candidate models:

1. Model **MM**: The simple Michaelis-Menten kinetic mechanism, which accounts only for substrate depletion.
2. Model **MM+pi**: The Michaelis-Menten mechanism accompanied by **p**roduct **i**nhibition.
3. Model **MM+ed**: The Michaelis-Menten mechanism accompanied by **e**nzyme **d**eactivation via the E.S complex.

4. Model **MM+pi+ed**: The Michaelis-Menten mechanism accompanied by product inhibition and by enzyme deactivation via the E.S complex.

The four candidate kinetic were each mathematically represented by an appropriate set of first-order ordinary differential equations automatically derived by the software package DynaFit [3, 4].

1.2.1. Model **MM**

$$\begin{array}{rcl:ll} & & & \rightarrow & \leftarrow \\ \mathrm{E+S} & \rightleftharpoons & \mathrm{E.S} & k_{\mathrm{a.S}} & k_{\mathrm{d.S}} \\ \mathrm{E.S} & \rightarrow & \mathrm{E+P} & k_{\mathrm{d.P}} & \end{array}$$

In this kinetic mechanism, $k_{\mathrm{a.S}} = 10^7\ \mathrm{M}^{-1}\mathrm{s}^{-1}$ is the second-order bimolecular association rate constant for the formation of the enzyme–substrate complex; it was held as a fixed parameter in the fit of the experimental data where SAM was the varied component; $k_{\mathrm{d.S}}$ (unit: s^{-1}) is the dissociation rate constant for the decomposition of the Michaelis complex into constituent components; and $k_{\mathrm{d.P}}$ (unit: s^{-1}) first-order rate constant for the formation of the monitored reaction product P. In the classical notation this particular rate constant would be identified as the *catalytic constant* "k_{cat}".

The corresponding system of differential equations automatically derived by DynaFit [4] is listed in Appendix B.1.1

1.2.2. Model **MM+pi**

$$\begin{array}{rcl:ll} & & & \rightarrow & \leftarrow \\ \mathrm{E+S} & \rightleftharpoons & \mathrm{E.S} & k_{\mathrm{a.S}} & k_{\mathrm{d.S}} \\ \mathrm{E.S} & \rightarrow & \mathrm{E+P} & k_{\mathrm{d.P}} & \\ \mathrm{E+P} & \rightleftharpoons & \mathrm{E.P} & k_{\mathrm{a.Pi}} & k_{\mathrm{d.Pi}} \end{array}$$

In this kinetic mechanism, $k_{\mathrm{a.Pi}} = 10^7\ \mathrm{M}^{-1}\mathrm{s}^{-1}$ is the second-order bimolecular association rate constant for the formation of the enzyme–product complex accounting for possible product inhibition; it was held as a fixed parameter; $k_{\mathrm{d.Pi}}$ (unit: s^{-1}) is the dissociation rate constant for the decomposition of the inhibited E.P complex into constituent components.

The corresponding system of differential equations automatically derived by DynaFit [4] is listed in Appendix B.1.2

1.2.3. Model **MM+ed**

$$\begin{array}{rcl:ll} & & & \rightarrow & \leftarrow \\ \mathrm{E+S} & \rightleftharpoons & \mathrm{E.S} & k_{\mathrm{a.S}} & k_{\mathrm{d.S}} \\ \mathrm{E.S} & \rightarrow & \mathrm{E+P} & k_{\mathrm{d.P}} & \\ \mathrm{E.S} & \rightarrow & \mathrm{F} & k_{\mathrm{ES}} & \end{array}$$

In this kinetic mechanism, k_{ES} is the first-order rate constant (unit: s^{-1}) for the irreversible denaturation of the Michaelis complex [1].

The corresponding system of differential equations automatically derived by DynaFit [4] is listed in Appendix B.1.3

1.2.4. *Model* **MM+pi+ed**

$$\begin{array}{rcll} & & & \rightarrow \quad \leftarrow \\ \mathrm{E}+\mathrm{S} & \rightleftharpoons & \mathrm{E.S} & : \quad k_{\mathrm{a.S}} \quad k_{\mathrm{d.S}} \\ \mathrm{E.S} & \rightarrow & \mathrm{E}+\mathrm{P} & : \quad k_{\mathrm{d.P}} \\ \mathrm{E}+\mathrm{P} & \rightleftharpoons & \mathrm{E.P} & : \quad k_{\mathrm{a.Pi}} \quad k_{\mathrm{d.Pi}} \\ \mathrm{E.S} & \rightarrow & \mathrm{F} & : \quad k_{\mathrm{ES}} \end{array}$$

This final kinetic mechanism combines the essential features of product inhibition and enzyme deactivation occurring simultaneously.

The corresponding system of differential equations automatically derived by DynaFit [4] is listed in Appendix B.1.4

1.2.5. *The regression equation*

The fitting function (model equation) for each individual data set is defined by Eqn (S1),

$$F(t) = F_0 + \sum_{i=1}^{n_S} r_i c_i(t) \qquad , \tag{S1}$$

where

$F(t)$	the experimental signal observed at time t
F_0	offset on the signal axis (a property of the instrument)
n_S	number of unique molecular species participating in the reaction mechanism
$c_i(t)$	the concentration of the ith species at time t
r_i	the molar response coefficient of the ith species

The concentrations of these molecular species at time t are computed from their initial concentrations (at time zero, $t = 0$) by solving an initial-value problem defined by a system of simultaneous first-order Ordinary Differential Equations (ODEs) listed above.

In the global fit [5] of combined progress reaction progress curves, the rate constants were treated as *globally* adjustable model parameters, as was the molar response coefficient of the fluorogenic product, P. In contrast, each kinetic trace in the global data set was associated with its own *locally* adjustable offset on the signal axis.

1.3. *Results*

1.3.1. *Representative example: Replicate R1*

Figure S2 represents in panel (a) the overlay of experimental data (replicate 1/3) spanning the first 20 minutes of the assay and the theoretical model curves generated from model **MM+pi+ed** using the best-fit values of rate constants listed in the table immediately below. The best-fit values of the locally adjusted baseline offsets (F_0 in Eqn (S1)) are omitted for brevity.

Model	Parameter	Value	Low	High
MM+Pi+Ed	$k_{\mathrm{d.S}}$, s^{-1}	8	6.07	10
	$k_{\mathrm{d.P}}$, s^{-1}	0.0301	0.0283	0.0319
	$k_{\mathrm{d.Pi}}$, s^{-1}	0.984	0.701	1.32
	k_{ES}, s^{-1}	0.000678	0.00063	0.000727

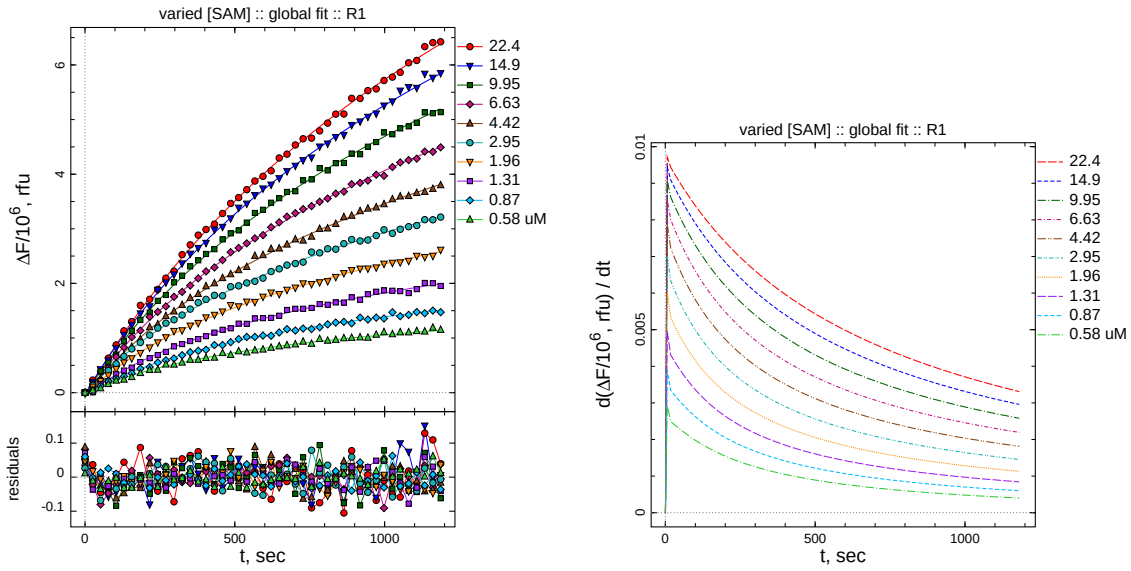

(a) (b)

Figure S2: Global nonlinear least-squares fit of combined control progress curves (zero inhibitor, varied SAM) to model **MM+pi+ed**, i.e., Michaelis-Menten mechanism accompanied by product inhibition and enzyme deactivation.

Panel (b) in *Figure S2* displays the changes in instantaneous reaction rates over the course of the first 20 minutes of the assay. The inventors of this particular enzyme assay [6] recommended a *linear* fit of the first 3 minutes, in order to determine initial reaction rates. This recommendation assumes that the reaction rate remains essentially unchanged over the given time period.

However, as can be seen in panel (b) of *Figure S2*, under the particular experimental conditions employed in this laboratory the instantaneous reaction rates change by as much as 25% – 33% between $t = 0$ and $t = 3$ min. This means that a linear fit of the 3-minute reaction progress is unsuitable and that a *nonlinear* regression procedure is necessary to quantify the enzymatic activity.

Note

The authors of the fluorescence assay [6] do not specify which variant of hNNMT they used. A relevant report [7] cited in the original publication presents both a wild-type (wt) variant and a triple-mutant (tm) variant used for crystallography. These enzymes have differential activity (relative activity of wt-hNNMT is 86% that of tm-hNNMT). The tm-hNNMT variant contains three mutations (K100A/E101A/E103A) designed to aid crystallization by reducing the entropy of surface-exposed residues in a loop distant from the active site [7]. These surface mutations could render a more stable protein, changing the rate of first-order decay of the Michaelis complex E.S. In our assays we used the wild-type variant (wt-hNNMT), but it is possible that wt-hNNMT could be more sensitive and unstable than tm-hNNMT.

1.3.2. Model discrimination analysis

Algorithm

The optimal mechanistic model for SAM substrate kinetic was selected by the software package DynaFit [4], using the following generally applicable model-selection criteria:

1. For a given candidate model to be accepted as plausible, the confidence intervals for all model parameters determined by the profile-t method of Bates and Watts [8–10] must be closed from both below and above at the given confidence level.
2. For a given plausible model to be identified as strongly preferred over other plausible candidate models, which also satisfy the acceptance criterion defined immediately above, one of two of the following criteria must hold:
   (a) *Non-continuous assays*: The differences in the Akaike Information Criterion (AIC) [11, 12] and the Bayesian Information Criterion (BIC) [12, 13] must be greater than 5.
   (b) *Continuous assays*: The differences in relative sum of squared deviations must be greater than 5%.

Note that the particular kinetic experiments conducted in this study belong into the category of continuous assays, where individual data points (time vs. fluorescence signal values) are *not* statistically independent and therefore the AIC and BIC model selection criteria cannot be used [14–16] in the usual manner.

Results

The auto-generated model discrimination analysis for replicates R1–R3 is shown in Appendix C.1.1–C.1.3. For all three independently replicated experiments, the preferred mechanistic model was **MM+pi+ed**, i.e., the Michaelis-Menten kinetic mechanism accompanied by both product inhibition and enzyme deactivation caused by a significant decay of the Michaelis complex ES. The results of model discrimination and parameter estimation are summarized in *Table S1*.

Note in *Table S1* that the best-fit values of microscopic rate constants are well reproduced among the three replicated measurements. In particular, the geometric standard deviation is

parameter	R1	R2	R3	GM	GSD
$k_{\mathrm{d.S}}$, s^{-1}	8.0	12.8	15.8	11.8	1.4
$k_{\mathrm{kd.P}}$, s^{-1}	0.030	0.038	0.041	0.036	1.2
$k_{\mathrm{kd.Pi}}$, s^{-1}	0.98	2.69	3.29	2.06	1.9
$k_{\mathrm{k.ES}}$, s^{-1}	0.00068	0.00054	0.00054	0.00058	1.1

Table S1: Substrate kinetic properties of SAM. GM = geometric mean from replicates R1–R3 ($n = 3$); GSD = geometric standard deviation.

lower than 2.0 for all four rate constants of interest, which means that the characteristic range of the relevant model parameter is within the factor of 2 in either direction (lower and higher relative to the geometric mean).

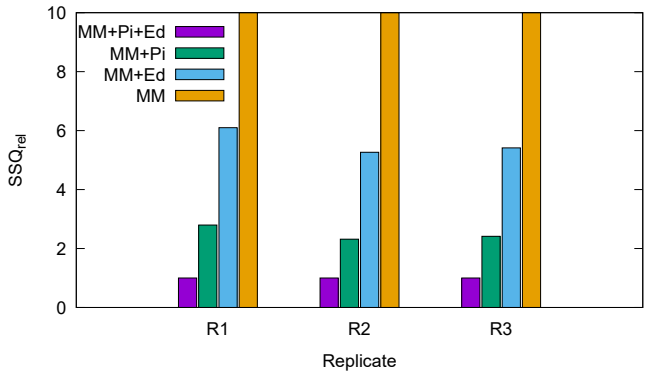

Figure S3: Relative residual sum of squared deviations obtained in the analysis of SAM substrate kinetic data in the fit to the four candidate fitting models. All three SSQ_{r} values for the model **MM** are all greater than 20 and are off-scale in this illustration.

The statistical preference for model **MM+pi+ed** is illustrated graphically in *Figure S3*. The relative sum-of-squares (SSQ_{r}) values were extracted from the detailed model discrimination report in Appendix C.1.1–C.1.3. The SSQ_{r} value for the runner-up model **MM+pi** (Michaelis-Menten kinetics accompanied by product inhibition) was at least twice as high as the SSQ_{r} for the optimal model **MM+pi+ed** (set to 1.0 by default).

The model **MM+ed** (Michaelis-Menten kinetics accompanied by enzyme deactivation) is associated with the same number of adjustable rate constants as the runner-up model **MM+pi** but, at the same time, model **MM+ed** produced a much higher value of $SSQ_{\mathrm{r}} > 5$. Thus enzyme deactivation alone cannot account for the deviation of SAM progress curves from the simple Michaelis-Menten kinetic mechanism.

The base model **MM** (pure Michaelis-Menten kinetics) was associated with extremely high values of $SSQ_{\mathrm{r}} > 20$ which, for clarity, are off-scale in *Figure S3* and it can therefore be unambiguously excluded from consideration. The deviation of the "best-fit" model curves generated from model **MM** were also clearly detectable by simple visual inspection of the experimental data overlaid on the model curves (results not shown).

It should be noted that strictly speaking the SSQ_r values displayed in *Figure S3* have only informative value, because the number of adjustable model parameters (rate constants) differs between candidate models. However, previously published empirical evidence [14] strongly suggests that $SSQ_r > 2.0$ is highly indicative of model discrimination power.

2. Substrate kinetic properties of quinoline

In this section we describe the determination of the apparent Michaelis constant of quinoline, $K_{mQ}^{(app)}$, at the screening concentration of [SAM] = 10 μM. This value is subsequently utilized to adjust the apparent inhibition constants to account for the competitive mechanism of inhibition of bisubstrate analogs.

2.1. Determination of initial rates

NNMT (100 nM) was assayed at 10 μM SAM in the absence of inhibitors. Quinoline concentration was varied from 10 to 120 μM. The individual reaction progress curves were fit to the integrated rate equation based on the Lambert Omega function [17] in order to determine initial reaction rates. See ref. [17] for further mathematical details. The requisite DynaFit [4] that was used to perform this kinetic analysis is listed in Appendix A.2. The results of fit are summarized graphically in *Figure S4*, for replicate 1/3.

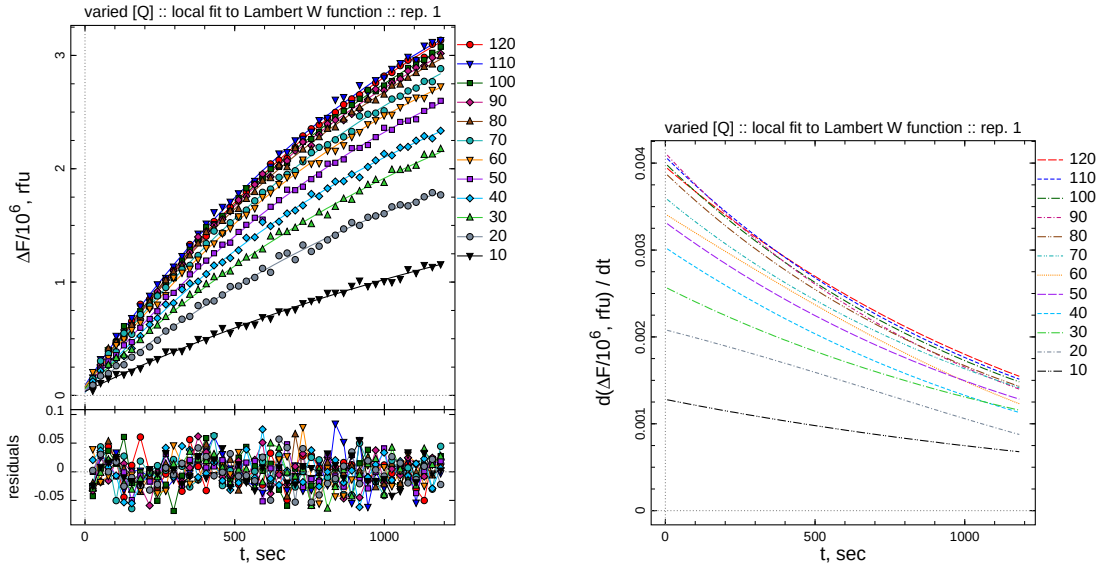

(a) Data and model overlay

(b) Instantaneous reaction rates

Figure S4: Least-squares fit of individual progress curves ("local" fit) to the theoretical model based on the Lambert Omega function [17] to determine initial reaction rates in dependence on quinoline concentration.

Note in *Figure S4* that the reaction time course is markedly nonlinear, as is evident from panel (b) displaying the instantaneous reaction rates. This nonlinearity necessitated the use of a

nonlinear regression model, as opposed to the standard linear fit of the "initial portion" in each individual reaction progress curve.

The goodness-of-fit to the Lambert Omega function [17] is satisfactory, as is evidenced by the random distribution of residuals of fit, bottom pane labeled "residuals" in panel (a) of *Figure S4*. The residual distribution is not showing any particular non-random pattern.

2.2. *Determination of the apparent Michaelis constant*

The initial reaction rates determined as described in section 2.1 were pooled, averaged, and fit to the Michaelis-Menten kinetic model represented symbolically as shown in the DynaFit [4] script listed in Appendix A.3. The results of fit are summarized graphically in *Figure S5*.

The best-fit parameter values are listed in the table immediately below. The "high" and "low" columns contain the upper and lower limits, respectively, of the 95% confidence interval determined by the profile-t method of Bates and Watts [8, 9].

#	parameter	initial	final ± std.err.	cv,%	low	high	note
1	K_{m}, μM	10	32.3 ± 1.5	4.6	29.1	35.8	
2	k_{cat}, s^{-1}	0.1	53.54 ± 0.84	1.6	51.76	55.47	

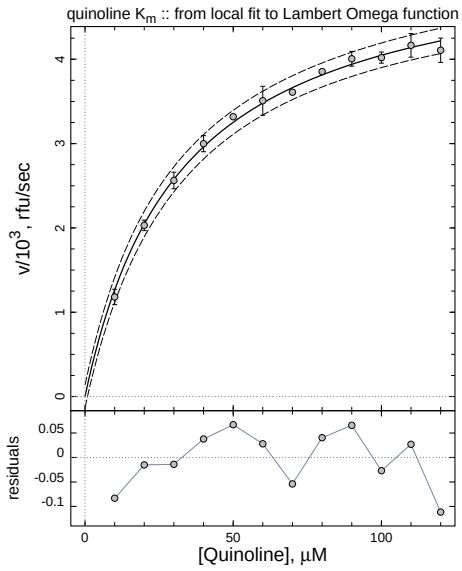

Figure S5: Least-squares fit of initial reaction rates from quinoline assay to the Michaelis-Menten reaction mechanism represented symbolically as shown in the DynaFit script listed in Appendix A.3. For details see text.

The results show that the apparent Michaelis constants of quinoline at the inhibitor screening concentration of [SAM] = 10 μM is equal to $K_{\mathrm{mQ}}^{(\mathrm{app})} = 32\ \mu$M. This result was utilized below in

our assessment of "apparent" vs. "true" inhibition constants determined as is explained in section 4.

3. A general steady-state initial rate equation for bisubstrate inhibitors

In this section we describe the use of the software package DynaFit [4] for the automatic derivation of the initial rate equation for any bisubstrate inhibitor acting on an enzyme that follows the "Ordered Bi Bi" kinetic mechanism [18], also known as "compulsory-order ternary-complex" mechanism [19]. The "Ordered Bi Bi" mechanism is relevant because Loring & Thompson [20] had recently demonstrated that a triple mutant of the recombinant human NNMT enzyme follows it.

The purpose of this derivation is to elucidate any possible difference between "apparent" inhibition constants [21] and "true" inhibition constants [22], in particular under tight-binding experimental conditions employed in this study.

3.1. Postulated kinetic mechanism

We assume that inhibition of NNMT follows the steady-state kinetic mechanism shown in the reaction scheme immediately below.

$$
\begin{array}{rcll}
\mathbf{A}+\mathbf{B} & \rightarrow & \mathbf{P}+\mathbf{Q} & \\
 & & & \rightarrow \quad \leftarrow \\
\mathrm{E}+\mathrm{A} & \rightleftharpoons & \mathrm{E.A} & : \quad k_1 \quad k_{-1} \\
\mathrm{E.A}+\mathrm{B} & \rightleftharpoons & \mathrm{E.X.Y} & : \quad k_2 \quad k_{-2} \\
\mathrm{E.X.Y} & \rightarrow & \mathrm{E.Q}+\mathrm{P} & : \quad k_3 \\
\mathrm{E.Q} & \rightarrow & \mathrm{E}+\mathrm{Q} & : \quad k_4 \\
\mathrm{E}+\mathrm{I} & \rightleftharpoons & \mathrm{E.I} & : \quad k_5 \quad k_{-5}
\end{array}
$$

In this mechanistic scheme, **A** and **B** represent SAM and quinoline, respectively. In the first step, SAM (**A**) attaches to the free enzyme, E. In contrast, quinoline (**B**) does not interact with the free enzyme but binds instead only to the binary complex E.A. This is according to the results of a mechanistic study previously reported in ref. [20].

The symbol "E.X.Y" stands for the ternary complex in both its isomeric incarnations (i.e., $EAB \rightleftharpoons EPQ$ in the frequently used notation). The ternary complex releases methyl-quinoline (**P**) as the first product and finally SAH (**Q**) is released to complete the catalytic cycle and regenerate the free catalyst, E.

We assume that in the fifth step characterized by rate constants k_5 and k_{-5} the inhibitor I binds to the free enzyme E (i.e., the apoenzyme), and that this is the only interaction between the inhibitor and the enzyme. This assumption is based on the fact that by definition bisubstrate analog inhibitors physically occlude the binding sites for both substrates and therefore when the inhibitor is bound neither of the substrates and/or products can bind at the same time.

In the input file for the software package DynaFit [4], the kinetic mechanism shown above is represented by using the following notation:

```
[mechanism]
   reaction A + B ---> P + Q
   modifiers I
   E + A <==> E.A       :  k1    k-1
```

```
   E.A + B <==> E.X.Y    :  k2    k-2   ;   E.X.Y is "(EAB <=> EPQ)"
   E.X.Y ---> E.Q + P    :  k3
   E.Q ---> E + Q        :  k4
   E + I <==> E.I        :  k5    k-5
```

3.2. The steady-state rate equation

We used the software package DynaFit [4] to derive the relevant algebraic form of the "Morrison equation" [23] corresponding to the inhibition mechanism listed above in section 3.1. The requisite DynaFit script is listed below:

```
[task]
   task = derive
   data = rates
   approximation = king-altman
[mechanism]
...
... (any arbitrary kinetic mechanism; see the example above)
...
[output]
   directory ./project/NNMT/01/derive/output
[settings]
{KingAltmanCleland}
   OutputSaturationEquations = y
   OutputMorrisonEquation = y
[end]
```

Note that the "Morrison equation" for tight-binding enzyme inhibition [21] is relevant because the enzyme concentration in our inhibitor screening assay was typically 100 nM, while at the same time many of the inhibition constants were in the same range or even significantly lower (sub-nanomolar in several cases).

> **Note**
>
> Morrison, on advice from W. W. Cleland (see the Acknowledgement section in ref. [23]), did not actually derive a steady-state initial rate equation that applies to any particular kinetic mechanism. Rather, he derived a general "template" formula that applies to nearly all kinetic mechanisms of inhibition (except partial inhibition mechanisms and inhibition mechanisms involving higher that 1:1 stoichiometry). Nor did Morrison provide any example how his generic "template" formula could be specialized for any given inhibition mechanism. The software package DynaFit [4] does include an algorithm for precisely this type of specialization, such that an actual rate equation is formed from the generic "template" derived by Morrison [23].

When the DynaFit package was presented with the script file listed above, the software automatically derived the "Morrison equation" for the postulated inhibition mechanism, as is shown in the system of equations immediately below:

$$v = v_0 \frac{[\mathrm{E}]_0 - [\mathrm{I}]_0 - K_\mathrm{i}^{(\mathrm{app})} + \sqrt{([\mathrm{E}]_0 - [\mathrm{I}]_0 - K_\mathrm{i}^{(\mathrm{app})})^2 + 4\,[\mathrm{E}]_0\,K_\mathrm{i}^{(\mathrm{app})}}}{2\,[\mathrm{E}]_0} \tag{S2}$$

$$K_\mathrm{i}^{(\mathrm{app})} = \frac{d_0}{d_\mathrm{I}} \tag{S3}$$

$$d_\mathrm{I} = \frac{1}{K_\mathrm{dI}} + \frac{K_\mathrm{mA}[\mathrm{B}]_0}{K_\mathrm{dA}K_\mathrm{mB}K_\mathrm{dI}} \tag{S4}$$

$$v_0 = [\mathrm{E}]_0 \frac{N}{d_0} \tag{S5}$$

$$N = k_\mathrm{cat} \frac{[\mathrm{A}]_0[\mathrm{B}]_0}{K_\mathrm{dA}K_\mathrm{mB}} \tag{S6}$$

$$d_0 = 1 + \frac{[\mathrm{A}]_0}{K_\mathrm{dA}} + \frac{K_\mathrm{mA}[\mathrm{B}]_0}{K_\mathrm{dA}K_\mathrm{mB}} + \frac{[\mathrm{A}]_0[\mathrm{B}]_0}{K_\mathrm{dA}K_\mathrm{mB}} \tag{S7}$$

$$k_\mathrm{cat} = \frac{k_3k_4}{k_4 + k_3} \tag{S8}$$

$$K_\mathrm{mA} = \frac{k_3k_4}{k_1\,(k_4 + k_3)} \tag{S9}$$

$$K_\mathrm{mB} = \frac{k_4\,(k_{-2} + k_3)}{k_2\,(k_4 + k_3)} \tag{S10}$$

$$K_\mathrm{dA} = \frac{k_{-1}}{k_1} \tag{S11}$$

$$K_\mathrm{dI} = \frac{k_{-5}}{k_5} \tag{S12}$$

The above system of equations, auto-generated by the DynaFit software package, can be rearranged to express the apparent inhibition constant in a more compact form as is shown in Eqn (S13).

$$K_\mathrm{i}^{(\mathrm{app})} = K_\mathrm{dI} \frac{K_\mathrm{dA}K_\mathrm{mB} + K_\mathrm{mB}[\mathrm{A}]_0 + K_\mathrm{mA}[\mathrm{B}]_0 + [\mathrm{A}]_0[\mathrm{B}]_0}{K_\mathrm{dA}K_\mathrm{mB} + K_\mathrm{mA}[\mathrm{B}]_0} \tag{S13}$$

Eqn (S13) can be profitably analyzed in terms of the expected inhibition patterns (competitive, uncompetitive, noncompetitive, mixed-type) with respect to each of the two substrates. The limits of $K_\mathrm{i}^{(\mathrm{app})}$ at either $[\mathrm{A}]_0$ or $[\mathrm{B}]_0$ approaching zero are shown in Eqns (S14)–(S15).

$$\lim_{[\mathrm{A}]_0 \to 0} K_\mathrm{i}^{(\mathrm{app})} = K_\mathrm{dI} \qquad \text{noncompetitive w.r.t. B} \tag{S14}$$

$$\lim_{[\mathrm{B}]_0 \to 0} K_\mathrm{i}^{(\mathrm{app})} = K_\mathrm{dI}\left(1 + \frac{[\mathrm{A}]_0}{K_\mathrm{dA}}\right) \qquad \text{competitive w.r.t. A} \tag{S15}$$

The assignment of competitive vs. noncompetitive patterns can be made in analogy to single-substrate systems analyzed by Cha [22]. According to Cha's analysis, the apparent inhibition constant for a competitive inhibitor will be higher than the "true" inhibition constant by the factor of $(1 + [\mathrm{S}]_0/K_\mathrm{M})$ (cf. [22, Eqn. (7)]). In contrast, the apparent inhibition constant for a noncompetitive inhibitor in a single-substrate system will not depend on the substrate concentration at all (cf. [22, Eqn. (9)]).

However, please note one important difference between Cha's Eqn (7) published in [22], including the multiplication factor $(1 + [\mathrm{S}]_0/K_\mathrm{M})$, and our Eqn (S15), including the multiplication factor $(1 + [\mathrm{A}]_0/K_\mathrm{dA})$. In Cha's case, the multiplication factor involves the *Michaelis constant* of the (in his case, single) substrate, whereas in our case the multiplication factor involves the *dissociation equilibrium constant* of the first attached substrate. Recall that Michaelis constants are always complex quantities encompassing many microscopic rate constants appearing in the given kinetic mechanism, whereas the dissociation equilibrium constant is always a simple ratio of the *off* rate constant divided by the *on* rate constant.

Taylor [24] derived a steady-state initial rate equation for a classical (as opposed to tight-binding) inhibitor interacting exclusively with the free enzyme in a bisubstrate system following the "Ordered Bi Bi" mechanism. The published algebraic derivation confirmed that such an inhibitor will show a *competitive* kinetic pattern with respect to the *first* attached substrate, and a *noncompetitive* inhibition pattern with respect to the *second* attached substrate (cf. [24, Eqns. 6.9 and 6.10, p. 74]).

The main purpose of the theoretical analysis presented in this section was as follows.

- All bisubstrate analog inhibitors (under either tight-binding or classical experimental conditions) acting on an enzyme following the "Ordered Bi Bi" mechanism are noncompetitive with respect to the second attached substrate, in this case quinoline.
- Therefore, quinoline concentration in the NNMT assay has no effect on the apparent inhibition constant, $K_\mathrm{i}^{(\mathrm{app})}$.
- The apparent inhibition constant of all bisubstrate analog inhibitors acting on an enzyme following the "Ordered Bi Bi" mechanism depend only on the concentration of the first attached substrate, such that $K_\mathrm{i}^{(\mathrm{app})} = K_\mathrm{d}(1 + [\mathrm{A}]_0 k_\mathrm{on}/k_\mathrm{off})$, where k_on and k_off are microscopic rate constants for the first attached substrate interacting with the apoenzyme.
- Therefore, if we can construct a suitable differential-equation model for the reaction progress explicitly incorporating k_on and k_off for the first attached substrate, the resulting best-fit values of the on/off rate constants for the (competitive) inhibitor will be the "true" rate constants and therefore their ratio will also be the "true" inhibition constant, i.e., the dissociation constant of the enzyme–inhibitor complex.

The above theoretical analysis proves that the best-fit values of on/off rate constants for bisubstrate analog inhibitors reported in this paper are "true" and not "apparent" rate constants. Therefore the off/on rate constant ratio is also the "true" inhibition constant, as opposed to an apparent inhibition constant.

4. Inhibition kinetics: Theory and methods

4.1. Raw experimental data

Upon simple visual examination, the raw experimental data from our NNMT inhibition assays could be qualitatively classified into at least two distinct categories:

1. Strong nonlinearity due to "slow-binding" inhibition detectable by visual inspection.
2. Moderate nonlinearity, possibly with a "slow-binding" component and/or due to other factors.

In the first category were numerous kinetic experiments that resulted in prominently nonlinear reaction progress curves. The observed deviations from a linear time course were visibly more prominent than the gradual nonlinearity observed in positive control experiments, conducted in the absence of inhibitors (see for example *Figure S1*). This pronounced additional nonlinearity strongly suggests *time-dependent i.e. "slow-binding" inhibition* [25, 26].

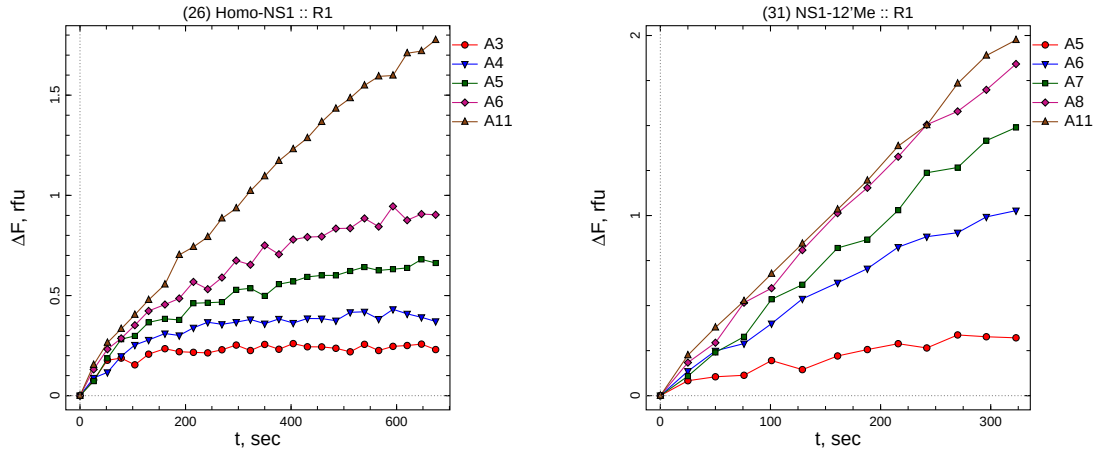

(a) (b)

Figure S6: Raw experimental data from inhibition assays of NNMT. (a) – Compound **26**, replicate 1, 33 nM NNMT; (b) – Compound **31**, replicate 1, 100 nM NNMT. For details see text.

A typical example of clearly detectable "slow-binding" inhibition is illustrated in the left-hand panel (a) of *Figure S6* (compound **26**, replicate R1). The data set labels correspond to individual wells on a 96-well plate. The trace in well **A11** was obtained in the absence of inhibitor; wells **A3** – **A6** correspond to inhibitor concentrations 293, 196, 131, and 87 nM, respectively.

The characteristic "slow-binding" inhibition pattern is most prominently illustrated by the kinetic trace labeled **A4** (blue triangles down). The slope of a tangent to the progress curve drawn at time zero (i.e., the initial reaction rate at [I] = 196 nM) would very closely approximate the uninhibited rate (i.e., the initial reaction rate at [I] = 0). The instantaneous rate (slope) subsequently changes over time, until, at approximately $t = 5$ min, the reaction progress curve becomes nearly horizontal, corresponding to nearly complete inhibition. Thus, in this particular case, the inhibitory effect gradually developed over the course of approximately 5 minutes (hence "slow-binding").

A typical example of the other kind of progress curves, less clearly interpretable, is illustrated in the right-hand panel (b) of *Figure S6* (compound **31**, replicate R1). As before, the trace in well **A11** was obtained in the absence of inhibitor; wells **A5** – **A8** correspond to inhibitor concentrations 317, 100, 32, and 10 nM, respectively.

In this particular case, all reaction progress curves are again somewhat nonlinear, but it is no longer possible to conclude – simply upon visual examination – whether the observed nonlinearity is due to "slow-binding" inhibition or merely due to the slight curvature that is also seen in the substrate-only ([I] = 0) control curve. In fact, most reaction progress curves we observed belong into this second category.

4.2. Theoretical models

The experimental data from inhibition assays, exemplified in *Figure S6*, were subjected to global nonlinear regression analysis. In this section we describe the general form of the regression equation; three alternate mechanistic models and the corresponding systems of differential equations; two alternate treatment of fixed vs. adjustable model parameters; and a model-discrimination algorithm that was utilized to select the most plausible candidate kinetic mechanism for each particular inhibitor.

4.2.1. The regression equation

All progress curves arising from a given dose-response experiment, including the control progress curves obtained at zero inhibitor concentration, were combined and fit to Eqn (S1). However, the concentrations of reacting species $c_i(t)$ were computed by solving a system of first-order ordinary differential equations (ODE) corresponding to one of several reaction mechanisms discussed below. Each ODE system was automatically derived by the DynaFit software package [4].

In order to properly characterize a variety of distinct features we identified in the overall shape of the reaction progress curves (see *Figure S6*), we have constructed three alternate regression models for each globally combined set of enzymatic progress curves.

4.2.2. Model **R1S***: "slow-binding"*

$$\begin{array}{rcll} & & & \rightarrow \quad \leftarrow \\ \mathrm{E+S} & \rightleftharpoons & \mathrm{E.S} & : \quad k_{\mathrm{a.S}} \quad k_{\mathrm{d.S}} \\ \mathrm{E.S} & \rightarrow & \mathrm{E+P} & : \quad k_{\mathrm{d.P}} \\ \mathrm{E+P} & \rightleftharpoons & \mathrm{E.P} & : \quad k_{\mathrm{a.Pi}} \quad k_{\mathrm{d.Pi}} \\ \mathrm{E.S} & \rightarrow & \mathrm{F} & : \quad k_{\mathrm{ES}} \\ \mathrm{E+I} & \rightleftharpoons & \mathrm{E.I} & : \quad k_{\mathrm{a.I}} \quad k_{\mathrm{d.I}} \end{array}$$

The first four steps in the above mechanism are exactly identical to model **MM+pi+ed** for SAM substrate kinetics (see section 1.2.3. The last step listed above describes a reversible binding of inhibitor I to the enzyme E to form the non-covalent enzyme-substrate complex E.I. The above mechanism is described mathematically by the ODE system of Eqns (S36)–(S43).

Importantly, when utilizing the above model **R1S** to fit the time-course of NNMT inhibition, both newly introduced rate constants, namely, $k_{\mathrm{a.I}}$ that quantifies the enzyme–inhibitor association and $k_{\mathrm{d.I}}$ that describes the dissociation of the enzyme–inhibitor complex, are treated as adjustable model parameters.

4.2.3. Model **R1F***: "fast-binding"*

The molecular mechanism underlying this fitting model is exactly identical to the symbolic scheme shown in section 4.2.2 above. Thus, the corresponding system of differential equations is also exactly identical. The only important difference is that in model **R1F** we assumed that the intermolecular association between the enzyme and the inhibitor is instantaneous, or nearly instantaneous on the time scale of the experiment.

This "fast-binding" assumption was implemented by setting the bimolecular association rate constants $k_{a.I}$ to the arbitrarily chosen value of 10^7 $\mathrm{M}^{-1}\mathrm{s}^{-1}$, or 10 $\mu\mathrm{M}^{-1}\mathrm{s}^{-1}$. This particular *diffusion controlled* value of $k_{a.I}$ was chosen on the basis well established precedents in the literature.[27, 28].

4.2.4. Model **C1***: "irreversible" binding*

In a preliminary round of kinetic analyses (results not shown) we identified certain experimental data sets, for which the lower limit of the enzyme–inhibitor dissociation constant $k_{d.I}$ could not be determined at the given confidence level, because it was essentially too low to measure reliably.

In order to assign an acceptable theoretical model to such exceptional data sets, we have included in our statistical model discrimination analysis the irreversible binding mechanism shown immediately below:

$$\begin{array}{rcl:l:cc} & & & & \rightarrow & \leftarrow \\ \mathrm{E}+\mathrm{S} & \rightleftharpoons & \mathrm{E.S} & : & k_{a.S} & k_{d.S} \\ \mathrm{E.S} & \rightarrow & \mathrm{E}+\mathrm{P} & : & k_{d.P} & \\ \mathrm{E}+\mathrm{P} & \rightleftharpoons & \mathrm{E.P} & : & k_{a.Pi} & k_{d.Pi} \\ \mathrm{E.S} & \rightarrow & \mathrm{F} & : & k_{ES} & \\ \mathrm{E}+\mathrm{I} & \rightarrow & \mathrm{E.I} & : & k_{a.I} & \end{array}$$

According to this particular theoretical reaction scheme, the enzyme–inhibitor association is formally irreversible. However, this does *not* mean that the given inhibitor is being covalently attached to the enzyme target. Indeed it is reasonable to assume that all 35 inhibitors in our compound collection are reversible as opposed to covalent inhibitors. Instead, the true meaning and utility of model **C1** is to express the fact that the lower limit of the confidence interval for the dissociation constant $k_{d.I}$ cannot be reached at the given confidence level.

4.3. Two methods of handling substrate kinetic constants

Our basic approach was to treat the *substrate* kinetic parameters for SAM as fixed parameters in the global analysis of the *inhibition* data. This treatment would ideally involve all floating substrate rate constants $k_{d.S}$, $k_{d.P}$, $k_{d.Pi}$ and k_{ES} that appear in the theoretical model **MM+pi+ed** described in section 1.2.4.

However, the complete collection of inhibition data consists of 105 plate-reader data sets obtained over an approximately six month period. Such extended period of time suggests that the kinetic properties of the enzyme might have changed, however subtly, over the course of time. For this reason, in the global fit of inhibition data we employed two different methods of analysis.

4.3.1. Method A: Fixed "k_{cat}"

According to this method, *all* substrate-related rate constants enumerated above, including in particular the "k_{cat}" equivalent labeled $k_{d.P}$ in the mechanistic scheme, were treated as fixed model parameters. The only adjustable rate constants were those related to inhibitor association and/or dissociation.

Additionally, in this method of analysis, we chose to also optimize the molar response coefficient of the fluorogenic product, r_P in Eqn (S1). This choice was necessitated by the fact that the kinetics work was performed on two different plate-reader instruments, which had distinct sensitivity characteristics.[4] Finally, the list of adjustable model parameters included all baseline offsets on the signal axis, F_0 in Eqn (S1).

4.3.2. Method B: Adjustable "k_{cat}"

According to this alternate method, all substrate-related rate constants enumerated above, *except* the "k_{cat}" equivalent labeled $k_{d.P}$ in the mechanistic scheme, were treated as fixed model parameters. Also treated as adjustable in the regression Eqn (S1) were rate constants pertaining to inhibitor association and/or dissociation.

The auxiliary model parameters r_P, i.e., the molar responses coefficient of the reaction product, and F_0, i.e., the offsets on the signal axis, were treated in the same way as in Method A described above.

5. Inhibition kinetics: Results

In this section we first present representative examples of global fit and model discrimination for three types of kinetic behavior encountered in this study:

1. Inhibitors that display "fast" or instantaneous binding on the time-scale of the experiment.
2. Inhibitors that display prominent "slow" binding, or time dependence, clearly discernible even by simple visual examination of raw kinetic data.
3. Kinetic experiments that revealed that there is a "slow" component to enzyme-inhibitor interactions only upon close scrutiny.

We also report potency ranking of NS1 analogs obtained by two alternate data-analysis methods.

5.1. Example 1: Compound **18***, "fast-binding"*

Compound **18** was identified as one of the few compounds in this collection of 35 NNMT inhibitors that show very clear preference for the "fast-binding" inhibition mechanism **R1F**. This is illustrated in *Figure S7*. The inhibitor concentrations in well A2 through A10 were 100, 31.6, 10, 3.16, 1, 0.316, 0.1, 0.0316, and 0.01 μM, respectively. The experimental traces marked as A11 and A12 represent the negative control wells, where the inhibitor was absent.

The left-hand panel (a) in *Figure S7* shows the overlay of the experimental data points (various symbols) and the best-fit theoretical model curves, which were generated from the ODE

[4] The two plate-reader instruments were the same model, from the same manufacturer, but displayed different sensitivity because of subtle mechanical and/or optical variation.

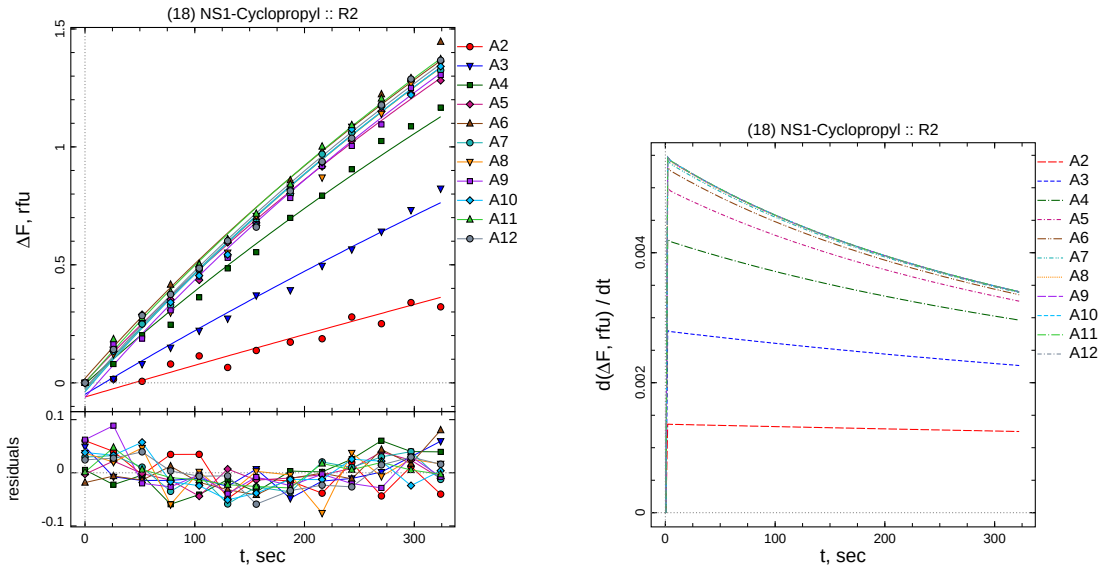

(a) (b)

Figure S7: Global nonlinear least-squares fit of combined control progress curves from the inihibition assay of compound **18**. For details see text.

system listed in Appendix B.2.1. The right-hand panel (b) displays the plot of instantaneous reaction rates, i.e., derivatives of the experimental model curves shown in panel (a) with respect to time. Note that the the reaction rate at time zero varies prominently with the inhibitor concentration. Such strong dependence of initial rates on the inhibitor concentration is a kinetic signature of the "fast-binding" mechanism **R1F**.

5.1.1. Model discrimination analysis

With regard to model discrimination analysis in the case of compound **18**, as a typical example of "fast-binding" inhibitors in this compound collection, the detailed results auto-generated by the DynaFit software are listed in Appendix C.2. The two most salient observations that emerge on the basis of the detailed results are as follows:

1. The "fast-binding" kinetic model **R1F** and the "slow-binding" model **R1S** produced exactly identical residual sums of squares. However, model **R1F** is by definition associated with fewer adjustable parameters (i.e., the dissociation rate constant $k_{d.I}$ only) in comparison with model **R1S** (involving two adjustable rate constant, $k_{a.I}$ and $k_{d.I}$).
2. The confidence intervals for $k_{a.I}$ and $k_{d.I}$ in the "slow-binding" model **R1S** were half-opened from above as determined by the profile-t method of Bates and Watts [8–10] ($\Delta SSQ_r = 1\%$ according to the empirical method proposed by Johnson [14–16]). This is illustrated in *Figure S8*.

Either of the first two observations listed above would be sufficient to exclude the "slow-binding" model **R1S** in favor of the "fast-binding" model **R1F**. However, the confidence interval

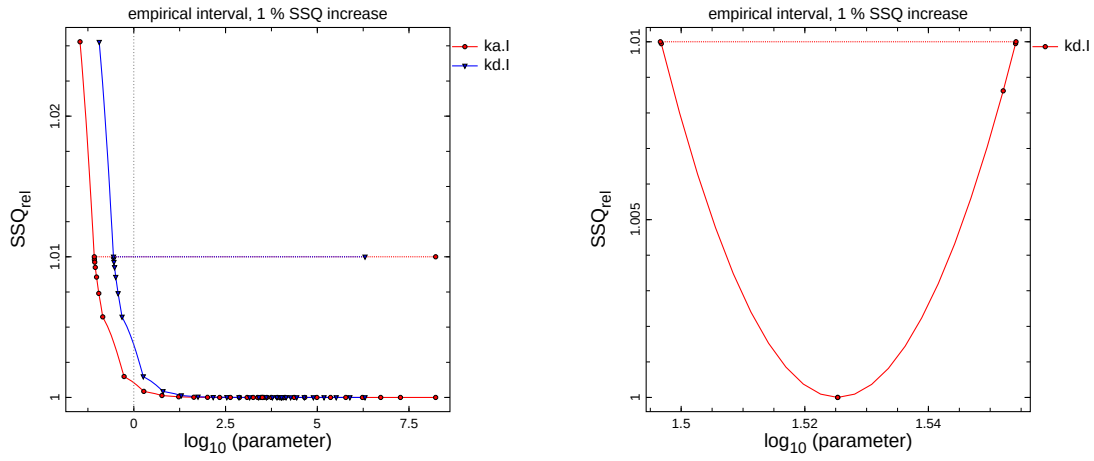

(a) (b)

Figure S8: Confidence interval profiles for rate constants determined by the profile-*t* method of Bates and Watts [8–10] in the fit of compound **18** inhibition data. (a) "Slow-binding" model **R1S**; (b) "fast-binding" model **R1F**.

profiles shown in *Figure S8* are particularly informative. Note in the left-hand panel (a) of *Figure S8* that the confidence interval profiles for either $k_{a.I}$ or $k_{d.I}$ display not even the slightest hint of a minimum on the least-squares hyper-surface. Only the lower limits for both rate constants could be determined at the $\Delta SSQ_r = 1\%$ confidence level.

5.1.2. Model-invariance of the inhibition constant

Another important observation that emerges from examination of the detailed model-selection results listed in Appendix C.2 is that the the best-fit values of the inhibition constant, defined as the ratio of the dissociation and association rate constants $K_i \equiv k_{d.I}/k_{a.I}$, is invariant with respect to the choice of the fitting model. In other words, no matter which fitting model is considered as the "true" mechanism, either the fast-binding mechanism **R1F** or the slow-binding mechanism **R1S**, the inhibition constant comes out the same.

Note in the table labeled *Intermediate results: Kinetic constants* in Appendix C.2 that the best-fit values of the association and dissociation rate constants associated with the "slow-binding" model **R1** are $k_{a.I} = 5.35 \times 10^6\ \mu M^{-1}s^{-1}$ and $k_{d.I} = 1.8 \times 10^7\ s^{-1}$. The associated formal standard errors in the *StdErr* column are extremely large, corresponding to the coefficient of variation (*CV* column) greater than 5000%. Thus, these particular "best-fit" values of $k_{a.I}$ and $k_{d.I}$ should be ignored as invalid.

However, also note that the ratio of the two (individually invalid) rate constants, $K_i \equiv k_{d.I}/k_{a.I} = 1.8 \times 10^7/5.35 \times 10^6 = 3.35\ \mu M$, is exactly identical to the equivalent value of K_i determined from "fast-binding" kinetic model **R1F**.

In particular, the third row of the *Kinetic constants* table in Appendix C.2 lists $k_{d.I} = 33.5 \times 10^7\ s^{-1}$ as the best-fit value within model **R1F**. Recall that, according to the assumptions inherent in this particular kinetic model, the *assumed* (fixed) value of the enzyme–inhibitor association rate constant is $k_{a.I} = 10\ \mu M^{-1}s^{-1}$. Thus, the "fast-binding" model results in $K_i \equiv k_{d.I}/k_{a.I} =$

$33.5/10 = 3.35$ μM, which is exactly the same result that would be obtained from the "slow-binding" model **R1S**.

5.2. Example 2: Compound **26***, "slow-binding"*

Compound **26** is an example of several compounds in this collection that displayed clear "slow-binding" behavior easily detectable even by simple visual inspection. This is illustrated in *Figure S9*. The inhibitor concentrations in well A5 through A10 were 130, 87, 58, 39, 26, and 17 nM, respectively. The enzyme concentration was 33 nM. The experimental traces marked as A11 and A12 represent the negative control wells, where the inhibitor was absent.

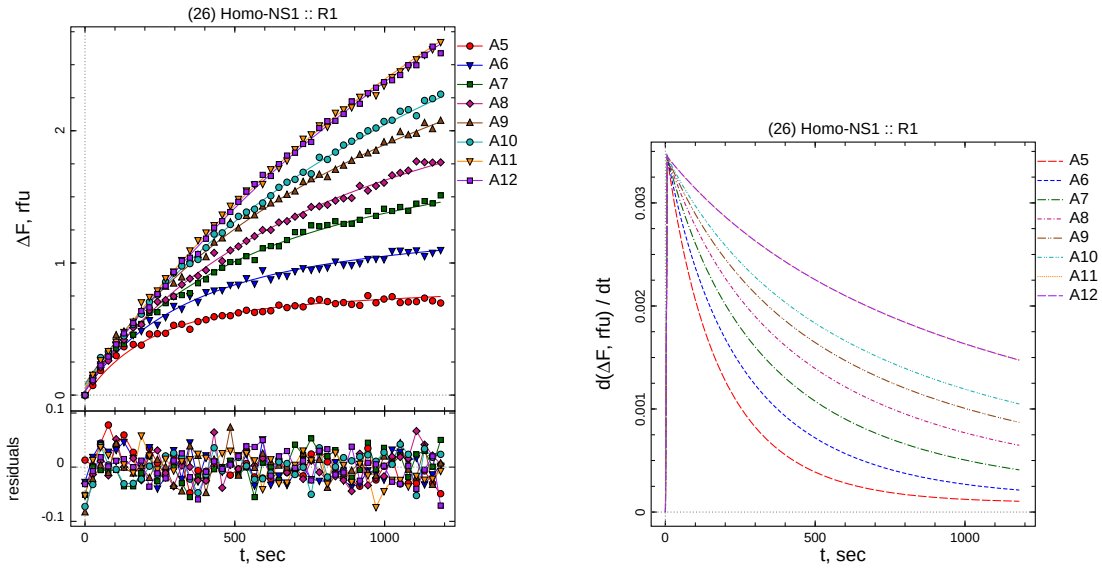

(a) (b)

Figure S9: Global nonlinear least-squares fit of combined control progress curves from the inhibition assay of compound **26**, replicate R1. For details see text.

The best-fit model curves displayed in *Figure S9* were generated by using Method A, in which the "k_{cat}" rate constant $k_{d.P}$ was fixed at the best-fit value determined in the analysis of SAM kinetic data as described in Section 1. Nevertheless, as can be seen from the left-hand panel (a) of *Figure S9*, the negative control progress curves (wells A11 and A12) shows nearly perfect agreement with the presumed substrate kinetic properties.

This agreement (a) theoretical model curves based on the assumed (fixed) values of substrate-related rate constants and (b) the experimental traces observed in the absence of inhibitor is especially remarkable, given that the substrate-alone progress curves (wells A11 and A12) are strongly nonlinear. This is illustrated by the fact that the instantaneous reaction rate observed at $[\mathrm{I}]_0 = 0$, in the right-hand panel of *Figure S9*, decreased by approximately 50% over the course of the 20-minute assay.

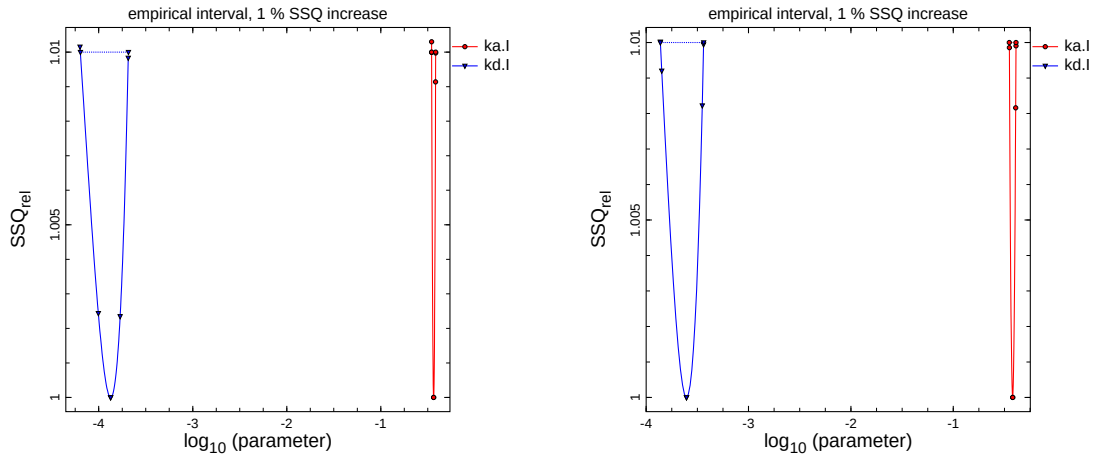

Replicate 1 Replicate 2

Figure S10: Confidence interval profiles for rate constants determined by the profile-*t* method of Bates and Watts [8–10] in the fit of compound **26** inhibition data.

5.2.1. Model discrimination analysis

With regard to model discrimination analysis in the case of compound **26**, as a typical example of "slow-binding" inhibitors in this compound collection, the detailed results auto-generated by the DynaFit software are listed in Appendix C.3. The most salient observations that emerge on the basis of the detailed results are as follows:

1. Table *Intermediate Results, Kinetic constants* in Appendix C.3: All three candidate fitting models ("slow-binding" **R1S**, "fast-binding" **R1F**, and "irreversible" **C1**) resulted in the confidence intervals for all relevant rate constants being closed from both above and below. Thus, on the basis of confidence intervals alone, it is not possible to decide in favor of either model.
2. Table *Final results, Information-theoretic criteria* in Appendix C.3: The "fast-binding" model **R1F** can be excluded on the basis of the fact that it is associated with much higher residual sum of squares ($SSQ_r \approx 7.475$) relative to the "irreversible" model ($SSQ_r \approx 1.037$) even though both models contain the same number of adjustable parameters ($n_P = 10$)[5]. However the "irreversible" binding model **C1** cannot be excluded from consideration because the relative sum of squares is only 3.7% higher than the slow, reversible binding model **R1S**. This value is lower than the 5% ΔSSQ_r cut-off we required for a model to be formally disqualified.

Thus, in the absence of any other information, the "slow-binding" and "irreversible" binding models would both remain equally plausible, although the reversible model **R1S** is nominally favored because it has a slightly lower residual sum of squares, by approximately 4%.

[5] The 10 adjustable model parameters for models **R1F** and **C1** consist of one rate constant, one globally optimized molar response coefficient, and eight locally optimized offsets on the signal axis (one per progress curve).

However, further support for the reversible "slow-binding" model **R1S** as opposed to the "irreversible" model **C1** comes from two different sources. First, the chemical structure of compound **26** does not appear to support the idea that the compound could bind covalently to the enzyme. Second, the preference for model **R1S** has been observed in all three independently replicated experiments.

5.2.2. Confidence intervals for inhibition rate constants

Also very well reproduced across replicates R1–R3 is the fact the the confidence intervals or inhibition rate constants $k_{a.I}$ (association of the enzyme and inhibitor) and $k_{d.I}$ (dissociation of the noncovalent enzyme–inhibitor complex) are closed from both above and below. This is illustrated in *Figure S10*.

Note in *Figure S10* that the best-fit values of the *on*-constant $k_{a.I}$ are particularly well replicated, as is indicated by the position of the minimum for $k_{a.I}$ on the least-squares hyper-surface. The best-fit values of the *off*-constant $k_{d.I}$ are less well replicated and differ approximately two-fold going from replicate R1 to replicate R3. Results for replicate R3 (not shown) were similar.

5.2.3. Distribution of enzyme species

The DynaFit software package [4] allows us to represent visually the distribution of various reacting species along the time-course of the enzymatic assay. In this case, this was arranged by inserting the following line of text into the appropriate DynaFit script:

```
[data]
...
   monitor E, E.S, E.I, F
...
```

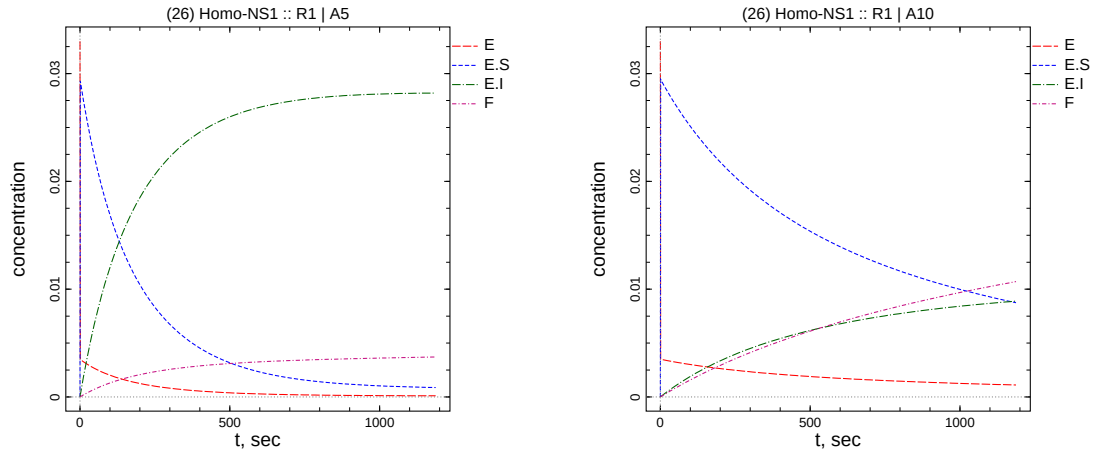

$[I]_0 = 130$ nM $[I]_0 = 17$ nM

Figure S11: Distribution of enzyme species in the inhibition assay of compound **26** at two different concentrations of the inhibitor. The enzyme concentration was 33 nM.

The results of this monitoring are displayed in *Figure S11*. According to model **R1S** and also using the assumed values of substrate-related rate constants determined in section 1, the distribution curves shown in *Figure S11* suggest that the enzyme–inhibitor complex is fully formed only at reaction times higher than approximately 10 minutes.

These and similar observations regarding the distribution of enzyme species should inform a thoughtful optimal design of kinetic experiments for the study of time-dependent enzyme inhibition, in particular with regard to the overall duration of the assay (in this case, at least 10-15 minutes).

5.3. Example 3: Compound **31**

The enzyme-kinetic results for compound **31** are typical for the majority of progress curves obtained in this study, in several respects:

1. The duration of the assay was only 5 minutes, as opposed to the more optimal 15 to 20 minutes.
2. The model discrimination analysis resulted in both the "slow-binding" and the "fast-binding" models being given nearly identical weight.
3. However, in all three replicates "slow-binding" model slightly dominated as measured by the residual sum of squares, SSQ_r.
4. Most importantly, the value of the inhibition constants defined as the ratio of rate constants $K_i \equiv k_{d.I}/k_{a.I}$ was virtually insensitive to which model ("fast" or "slow") was assumed to be operative.

In the case of compound **31**, and also most other compounds investigated in this study, it is quite challenging for a casual observer to detect that there is indeed a "slow-binding" component. This is illustrated in *Figure S12*. The inhibitor concentrations in well A5 through A10 were 316, 100, 36, 10, 3.6, and 1.0 nM, respectively. The nominal enzyme concentration was 100 nM. The experimental traces marked as A11 and A12 represent the negative control wells, where the inhibitor was absent.

Note in the right-hand panel (b) of *Figure S12* that it takes approximately 60 and 90 seconds for the enzyme–inhibitor complex to be fully formed. This fact is most clearly visible in the case of progress curve labeled A6 corresponding to 100 nM inhibitor. Only an experienced data analyst would probably detect the presence of this kinetic transient by simple visual examination of the raw data displayed in panel (a). However, most importantly, the slight transient feature is very well reproduced across all three independently replicated experiments.

5.3.1. Model discrimination analysis

With regard to model discrimination analysis in the case of compound **31**, the detailed results auto-generated by the DynaFit software are listed in Appendix C.4. The most salient observations that emerge on the basis of the detailed results are as follows:

1. The inhibition constant defined as the ratio $K_i \equiv k_{d.I}/k_{a.I}$ is largely invariant with respect to the presumed kinetic model ("slow" **R1S** or "fast" **R1F**).
2. The inhibition constant defined as the ratio $K_i \equiv k_{d.I}/k_{a.I}$ is also very well reproduced across the three independently replicated experiments. Both of the above observations are documented in *Table S2* below.

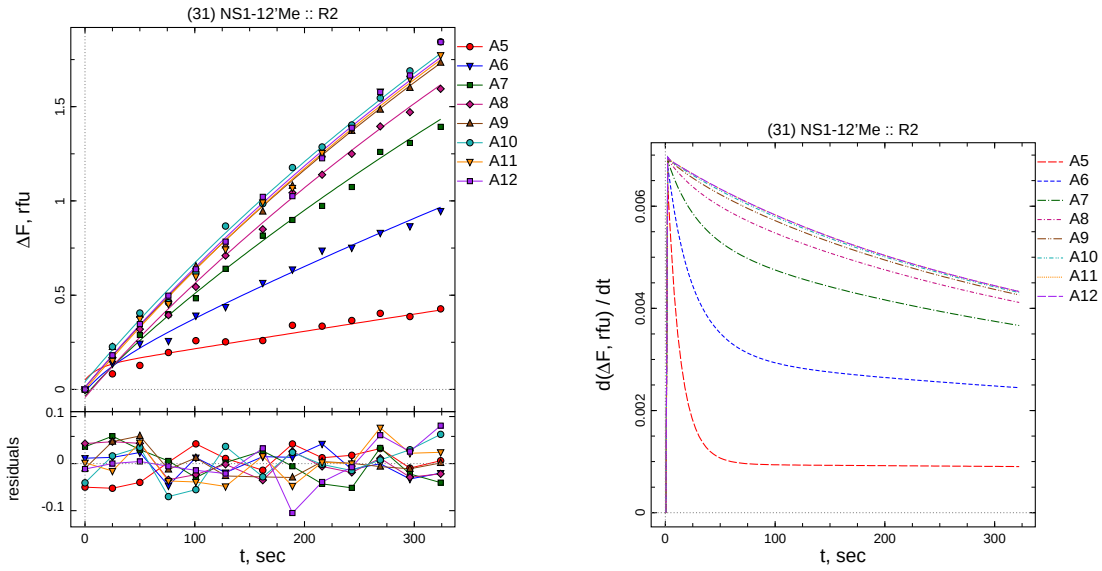

(a) (b)

Figure S12: Global nonlinear least-squares fit of combined control progress curves from the inhibition assay of compound **31**, replicate R2. For details see text.

model	$K_i \equiv k_{d.I}/k_{a.I}$, nM replicate 1	replicate 2	replicate 3
"slow-binding" **R1S**	3.3	3.8	2.5
"fast-binding" **R1F**	3.5	4.1	2.7

Table S2: Inhibition constants for compound **31** under the assumption of "slow" or "fast" binding, across three independent replicates.

5.3.2. Reproducibility and model-invariance of inhibition constants

The K_i values listed in *Table S2* were compiled from DynaFit-generated tables labeled *Intermediate results: Kinetic constants* in Appendix C.4. For example, the value $K_i = 3.3$ nM for model **R1S**, replicate 1, was computed as the ratio of $k_{d.I}/k_{a.I} = 0.0168/4.96 = 0.0033$ μM = 3.3 nM. Similarly, the value $K_i = 3.5$ nM for model **R1F**, replicate 1, was computed as the ratio of $k_{d.I}/k_{a.I} = 0.0348/10 = 0.00348$ μM = 3.48 nM. Note that in the case of the "fast" binding model **R1F** we assumed that the enzyme–inhibitor association is described by the diffusion-controlled rate constant $k_{a.I} = 10$ μM^{-1}s^{-1} = 10^7 M^{-1}s^{-1}.

5.4. Potency ranking of NS1 analogs

The tables below summarize the potency ranking for NS1 analogs obtained by the two methods of analysis, namely, Method A ("k_{cat}" rate constant fixed in the model) and Method B ("k_{cat}" rate constant optimized). In table headings, $pK_i = -\log_{10} K_i$ where K_i is in molar units (moles per liter).

5.4.1. Method A

rank	NS1 analog	cpd. no.	pK_i R1	pK_i R2	pK_i R3	aver. ± sdev.
1	Homo-NS1	**26**	9.90	9.62	10.00	9.84 ± 0.20
2	NS1-12'Cl	**33**	9.91	9.56	9.70	9.72 ± 0.18
3	NS1	**10**	9.27	9.47	9.42	9.38 ± 0.11
4	NS1-12'F	**30**	8.66	8.89	8.72	8.76 ± 0.12
5	NS1-12'CF3	**32**	8.54	8.68	8.57	8.60 ± 0.07
6	NS1-12'Me	**31**	8.48	8.43	8.61	8.50 ± 0.09
7	NS1-Alkane	**15**	8.37	8.37	8.46	8.40 ± 0.05
8	NS1-Pyr13'	**39**	8.38	8.40	8.36	8.38 ± 0.02
9	NS1-Pyr10'	**37**	8.15	8.21	8.28	8.21 ± 0.07
10	NS1-Pyr12'	**38**	8.21	8.05	8.10	8.12 ± 0.08
11	NS1-AminoAmide	**24**	7.84	7.88	7.85	7.86 ± 0.02
12	NS1-Methylenedioxy	**36**	7.50	7.56	7.51	7.52 ± 0.04
13	NS1-Pyr14'	**40**	7.43	7.48	7.52	7.48 ± 0.04
14	NS1-Benzolactam6	**34**	7.36	7.39	7.34	7.37 ± 0.03
15	NS1-Amine	**21**	7.32	7.31	7.33	7.32 ± 0.01
16		MS2734	7.15	7.13	7.16	7.15 ± 0.01
17	NS1-Urea	**25**	7.17	7.09	7.13	7.13 ± 0.04
18	NS1-Alkane 6'Epi	**16**	6.98	6.92	6.96	6.95 ± 0.03
19	NS1-6'Epi	**14**	6.85	6.88	6.97	6.90 ± 0.06
20	NS1-Sulfonamide	**29**	6.71	6.84	6.73	6.76 ± 0.07
21	Mini-NS1	**17**	6.63	6.59	6.56	6.59 ± 0.04
22	NS1-MethylEster	**23**	6.44	6.32	6.35	6.37 ± 0.06
23		MS2756	6.08	6.14	6.12	6.12 ± 0.03
24	NS1-Amide	**22**	6.01	6.06	6.00	6.02 ± 0.03
25	NS1-Benzolactam5	**35**	5.79	5.77	5.83	5.79 ± 0.03
26	NS1-Cyclopropyl	**18**	5.49	5.47	5.57	5.51 ± 0.05
27	NS1-Aminonaphthalene	**41**	5.54	5.48	5.48	5.50 ± 0.03
28	NS1-*p*Benzamide	**27**	5.28	5.30	5.30	5.29 ± 0.01
29		VH45	5.27	5.30	5.30	5.29 ± 0.02
30	NS1-Phenyl	**13**	4.96	4.94	5.03	4.98 ± 0.04
31	NS1-*o*Benzamide	**28**	4.81	4.77	4.79	4.79 ± 0.02
32	Desthia-SAH	**11**	4.72	4.76	4.76	4.75 ± 0.02
33	NS1-Carboxylic Acid	**20**	4.67	4.78	4.75	4.73 ± 0.06
34	NS1-Alkyne	**12**	4.37	4.34	4.31	4.34 ± 0.03
35	NS1-Desadenine	**19**	4.19	4.19	4.07	4.15 ± 0.07

5.4.2. Method B

rank	NS1 analog	cpd. no.	pK_i R1	pK_i R2	pK_i R3	aver. ± sdev.
1	NS1-12'Cl	**33**	9.88	9.59	9.70	9.72 ± 0.15
2	Homo-NS1	**26**	9.68	9.57	9.63	9.62 ± 0.05
3	NS1	**10**	9.23	9.36	9.32	9.30 ± 0.07
4	NS1-12'F	**30**	8.63	8.90	8.67	8.73 ± 0.15
5	NS1-12'CF3	**32**	8.51	8.68	8.55	8.58 ± 0.08
6	NS1-12'Me	**31**	8.44	8.39	8.57	8.47 ± 0.09
7	NS1-Alkane	**15**	8.31	8.32	8.36	8.33 ± 0.03
8	NS1-Pyr13'	**39**	8.29	8.32	8.28	8.30 ± 0.02
9	NS1-Pyr10'	**37**	8.11	8.19	8.22	8.17 ± 0.05
10	NS1-Pyr12'	**38**	8.17	8.00	7.99	8.05 ± 0.10
11	NS1-AminoAmide	**24**	7.74	7.78	7.79	7.77 ± 0.02
12	NS1-Methylenedioxy	**36**	7.46	7.54	7.46	7.49 ± 0.05
13	NS1-Pyr14'	**40**	7.38	7.45	7.51	7.45 ± 0.07
14	NS1-Benzolactam6	**34**	7.28	7.29	7.20	7.26 ± 0.05
15	NS1-Amine	**21**	7.25	7.22	7.25	7.24 ± 0.02
16	NS1-Urea	**25**	7.17	7.07	7.11	7.12 ± 0.05
17		MS2734	7.05	7.04	7.06	7.05 ± 0.01
18	NS1-Alkane 6'Epi	**16**	7.03	6.92	6.95	6.97 ± 0.05
19	NS1-6'Epi	**14**	6.87	6.87	6.99	6.91 ± 0.07
20	NS1-Sulfonamide	**29**	6.68	6.77	6.68	6.71 ± 0.05
21	Mini-NS1	**17**	6.62	6.59	6.53	6.58 ± 0.04
22	NS1-MethylEster	**23**	6.46	6.31	6.32	6.36 ± 0.08
23		MS2756	5.98	6.09	6.04	6.04 ± 0.06
24	NS1-Amide	**22**	5.97	5.99	5.98	5.98 ± 0.01
25	NS1-Benzolactam5	**35**	5.73	5.71	5.75	5.73 ± 0.02
26	NS1-Aminonaphthalene	**41**	5.52	5.40	5.38	5.43 ± 0.07
27	NS1-Cyclopropyl	**18**	5.38	5.37	5.47	5.40 ± 0.05
28	NS1-*p*Benzamide	**27**	5.22	5.24	5.25	5.24 ± 0.02
29		VH45	5.18	5.22	5.22	5.21 ± 0.02
30	NS1-Phenyl	**13**	4.88	4.88	4.94	4.90 ± 0.03
31	NS1-*o*Benzamide	**28**	4.71	4.69	4.72	4.71 ± 0.02
32	Desthia-SAH	**11**	4.65	4.67	4.68	4.67 ± 0.01
33	NS1-Carboxylic Acid	**20**	4.59	4.69	4.67	4.65 ± 0.06
34	NS1-Alkyne	**12**	4.39	4.33	4.24	4.32 ± 0.08
35	NS1-Desadenine	**19**	4.21	4.22	3.91	4.11 ± 0.17

5.4.3. Comparison of results

A comparison of results contained in the two summary tables listed immediately above reveals that the ranking of NS1 inhibitors by potency does not change upon going from Method A (fixed "k_{cat}") to Method B (optimized "k_{cat}") – as long as the statistical uncertainty of pK_i determinations is properly taken into account. This is true even though the *nominal order of potency* has changed from Method A to Method B in several cases. In particular, the "best" or most potent NS1 analog is compound **26** according to Method A, while at the same the "best" or most potent NS1 analog according to Method B is compound **33**. However, within both methods the pK_i values for both "top" ranked compounds are *identical within the margin or error*.

References

[1] P. Kuzmič, A. G. Peranteau, G. Garcia-Echeverria, D. H. Rich, Mechanical effects on the kinetics of the HIV proteinase deactivation, Biochem. Biophys. Res. Commun. 221 (1996) 313–7.

[2] M. Sadana, Biocatalysis - Fundamentals of Enzyme Deactivation Kinetics, Prentice-Hall, Englewood Cliffs, NJ, 1991.

[3] P. Kuzmič, Program DYNAFIT for the analysis of enzyme kinetic data: Application to HIV proteinase, Anal. Biochem. 237 (1996) 260–273.

[4] P. Kuzmič, DynaFit - A software package for enzymology, Meth. Enzymol. 467 (2009) 247–280.

[5] J. M. Beechem, Global analysis of biochemical and biophysical data, Meth. Enzymol. 210 (1992) 37–54.

[6] H. Neelakantan, V. Vance, H. L. Wang, S. F. McHardy, S. J. Watowich, Noncoupled fluorescent assay for direct real-time monitoring of nicotinamide N-methyltransferase activity, Biochemistry 56 (2017) 824–832.

[7] Y. Peng, D. Sartini, V. Pozzi, D. Wilk, M. Emanuelli, V. C. Yee, Structural basis of substrate recognition in human nicotinamide N-methyltransferase, Biochemistry 50 (2011) 7800–7808.

[8] D. M. Bates, D. G. Watts, Nonlinear Regression Analysis and its Applications, Wiley, New York, 1988.

[9] D. G. Watts, Parameter estimation from nonlinear models, Meth. Enzymol. 240 (1994) 24–36.

[10] I. Brooks, D. G. Watts, K. K. Soneson, P. Hensley, Determining confidence intervals for parameters derived from analysis of equilibrium analytical ultracentrifugation data, Meth. Enzymol. 240 (1994) 459–78.

[11] K. B. Burnham, D. R. Anderson, Model Selection and Multimodel Inference: A Practical Information-Theoretic Approach, 2nd Edition, Springer-Verlag, New York, 2002.

[12] J. I. Myung, M. A. Pitt, Model comparison methods, Meth. Enzymol. 383 (2004) 351–366.

[13] J. I. Myung, Y. Tang, M. A. Pitt, Evaluation and comparison of computational models, Meth. Enzymol. 454 (2009) 287–304.

[14] K. A. Johnson, Z. B. Simpson, T. Blom, Global Kinetic Explorer: A new computer program for dynamic simulation and fitting of kinetic data, Anal. Biochem. 387 (2009) 20–29.

[15] K. A. Johnson, Z. B. Simpson, T. Blom, FitSpace Explorer: An algorithm to evaluate multidimensional parameter space in fitting kinetic data, Anal. Biochem. 387 (2009) 30–41.

[16] K. A. Johnson, Fitting enzyme kinetic data with KinTek Global Kinetic Explorer, Meth. Enzymol. 467 (2009) 601–626.

[17] M. L. Reytor-Gonzalez, S. Cornell-Kennon, E. Schaffer, P. Kuzmič, An algebraic model for the determination of Michaelis-Menten kinetic parameters by global nonlinear fit of enzymatic progress curves, Anal. Biochem. 518 (2017) 16–24.

[18] W. W. Cleland, The kinetics of enzyme-catalyzed reactions with two or more substrates or products: I. Nomenclature and rate equations, Biochim. Biophys. Acta 67 (1963) 104–137.

[19] A. Cornish-Bowden, Fundamentals of Enzyme Kinetics, 4th Edition, Wiley-VCH Verlag GmbH & Co. KGaA, Berlin, 2012.

[20] H. S. Loring, P. R. Thompson, Kinetic mechanism of nicotinamide N-nethyltransferase, Biochemistry 57 (2018) 5524–5532.

[21] J. W. Williams, J. F. Morrison, The kinetics of reversible tight-binding inhibition, Meth. Enzymol. 63 (1979) 437–467.

[22] S. Cha, Tight-binding inhibitors. I. Kinetic behavior, Biochem. Pharmacol. 24 (1975) 2177–2185.

[23] J. F. Morrison, Kinetics of the reversible inhibition of enzyme-catalysed reactions by tight-binding inhibitors, Biochim. Biophys. Acta 185 (1969) 269–286.

[24] K. B. Taylor, Enzyme Kinetics and Mechanisms, Kluwer Academic Publishing, Dordrecht, 2002.

[25] J. F. Morrison, C. T. Walsh, The behavior and significance of slow-binding enzyme inhibitors, Adv. Enzymol. Related Areas Mol. Biol. 61 (1988) 201–301.

[26] S. Szedlacsek, R. G. Duggleby, Kinetics of slow and tight-binding inhibitors, Meth. Enzymol. 249 (1995) 144–180.

[27] T. E. Creighton, Proteins: Structures and Molecular Properties, 2nd Edition, W. H. Freeman, San Francisco, 1992.

[28] A. Fersht, Structure and Mechanism in Protein Science: A Guide to Enzyme Catalysis and Protein Folding, 3rd Edition, W. H. Freeman, New York, 1999.

Appendix

A. DynaFit scripts

This appendix contains the verbatim listing of example script input files for the software package DynaFit [4].

A.1. Global fit of SAM substrate kinetic data

The following DynaFit script file was used to fit one of the three replicates (in this case R1) of SAM substrate saturation data to the four candidate kinetic mechanisms displayed in sections 1.2.1–1.2.4, represented mathematically by the ODE system shown in Appendix B.1.1–B.1.4.

```
SAM substrate kinetics :: 4-way model discrimination
;_____________________________________________________________________________
[task]
   task = fit
   data = progress
   model = MM ? ; the simple Michaelis-Menten (MM) mechanism
[mechanism]
   E + S <==> E.S          :    ka.S    kd.S
   E.S ---> E + P          :    kd.P
[constants]
   ka.S = 10
   kd.S = {0.1, 1, 10, 100} ??
   kd.P = {0.00001, 0.0001, 0.001, 0.01, 0.1, 1} ??
[concentrations]
   E = 0.1
[responses]
   P = 1 ?
[data]
   directory ./project/NNMT/01/SAM/data
   sheet SAM-progress-R1.csv
   monitor E, E.S, E.P, F
graph varied [SAM] :: global fit :: R1
 ; column 3   | offset auto ? | conc S =  50.347    | label 50.3
 ; column 4   | offset auto ? | conc S =  33.564    | label 33.6
   column 5   | offset auto ? | conc S =  22.376    | label 22.4
   column 6   | offset auto ? | conc S =  14.918    | label 14.9
   column 7   | offset auto ? | conc S =  9.945    | label 9.95
   column 8   | offset auto ? | conc S =  6.63    | label 6.63
   column 9   | offset auto ? | conc S =  4.42    | label 4.42
   column 10  | offset auto ? | conc S =  2.947    | label 2.95
   column 11  | offset auto ? | conc S =  1.964    | label 1.96
   column 12  | offset auto ? | conc S =  1.31    | label 1.31
   column 13  | offset auto ? | conc S =  0.873    | label 0.87
   column 14  | offset auto ? | conc S =  0.582    | label 0.58 uM
[output]
   directory ./project/NNMT/01/SAM/output/fit-P-global-20min-4models-R1
[settings]
{Filter}
```

```
   XMax = 1200
{Output}
   XAxisLabel = t, sec
   YAxisLabel = {/Symbol D}F/10^6, rfu
{ConfidenceIntervals}
   SquaresIncreasePercent = 1
;_____________________________________________________________________________
[task]
   task = fit
   data = progress
   model = MM+Pi ? ; MM & product inhibition
[mechanism]
   E + S <==> E.S          :    ka.S    kd.S
   E.S ---> E + P          :    kd.P
   E + P <==> E.P          :    ka.Pi   kd.Pi
[constants]
   ka.S = 10
   kd.S = {0.1, 1, 10, 100} ??
   kd.P = {0.00001, 0.0001, 0.001, 0.01, 0.1, 1} ??
   ka.Pi = 10
   kd.Pi = {0.1, 1, 10, 100} ??
;_____________________________________________________________________________
[task]
   task = fit
   data = progress
   model = MM+Ed ? ; MM & enzyme deactivation
[mechanism]
   E + S <==> E.S          :    ka.S    kd.S
   E.S ---> E + P          :    kd.P
   E.S ---> F              :    k.ES
[constants]
   ka.S = 10
   kd.S = {0.1, 1, 10, 100} ??
   kd.P = {0.00001, 0.0001, 0.001, 0.01, 0.1, 1} ??
   k.ES = {0.0000001, 0.000001, 0.00001, 0.0001, 0.001, 0.01} ??
;_____________________________________________________________________________
[task]
   task = fit
   data = progress
   model = MM+Pi+Ed ? ; MM & product inhibition & ES --> F
[mechanism]
   E + S <==> E.S          :    ka.S    kd.S
   E.S ---> E + P          :    kd.P
   E + P <==> E.P          :    ka.Pi   kd.Pi
   E.S ---> F              :    k.ES
[constants]
   ka.S = 10
   kd.S = {0.1, 1, 10, 100} ??
   kd.P = {0.00001, 0.0001, 0.001, 0.01, 0.1, 1} ??
   ka.Pi = 10
   kd.Pi = {0.1, 1, 10, 100} ??
```

```
   k.ES = {0.0000001, 0.000001, 0.00001, 0.0001, 0.001, 0.01} ??
[end]
;_____________________________________________________________________
;_____________________________________________________________________
```

A.2. Local fit of quinoline substrate kinetic data

The following DynaFit script file was used to fit one of the three replicates (in this case R1) of quinoline substrate saturation data the integrated Michaelis-Menten rate equation, based on the Lambert Omega function [17], in order to determine the initial reaction rates.

```
;_____________________________________________________________________
[task]
   task = fit
   data = generic
   code = built-in
[equation]
   MichaelisMentenProgressKmKcat
[parameters]
   Eo = 0.1
[data]
   variable t
   directory ./project/NNMT/01/sub/Q/data
graph varied [Q] :: local fit to Lambert W function :: rep. 1
   sheet Q-progress-R1.csv
   column 3  | label 120
      parameter Fo = 0 ? (-100 .. +100), rP = 1 ?
      parameter Km = 1 ?, kcat = 0.1 ?, So = 120
   column 4  | label 110
      parameter Fo = 0 ? (-100 .. +100), rP = 1 ?
      parameter Km = 1 ?, kcat = 0.1 ?, So = 110
   column 5  | label 100
      parameter Fo = 0 ? (-100 .. +100), rP = 1 ?
      parameter Km = 1 ?, kcat = 0.1 ?, So = 100
   column 6  | label 90
      parameter Fo = 0 ? (-100 .. +100), rP = 1 ?
      parameter Km = 1 ?, kcat = 0.1 ?, So = 90
   column 7  | label 80
      parameter Fo = 0 ? (-100 .. +100), rP = 1 ?
      parameter Km = 1 ?, kcat = 0.1 ?, So = 80
   column 8  | label 70
      parameter Fo = 0 ? (-100 .. +100), rP = 1 ?
      parameter Km = 1 ?, kcat = 0.1 ?, So = 70
   column 9  | label 60
      parameter Fo = 0 ? (-100 .. +100), rP = 1 ?
      parameter Km = 1 ?, kcat = 0.1 ?, So = 60
   column 10  | label 50
      parameter Fo = 0 ? (-100 .. +100), rP = 1 ?
      parameter Km = 1 ?, kcat = 0.1 ?, So = 50
   column 11  | label 40
      parameter Fo = 0 ? (-100 .. +100), rP = 1 ?
```

```
      parameter Km = 1 ?, kcat = 0.1 ?, So = 40
   column 12  | label 30
      parameter Fo = 0 ? (-100 .. +100), rP = 1 ?
      parameter Km = 1 ?, kcat = 0.1 ?, So = 30
   column 13  | label 20
      parameter Fo = 0 ? (-100 .. +100), rP = 1 ?
      parameter Km = 1 ?, kcat = 0.1 ?, So = 20
   column 14  | label 10
      parameter Fo = 0 ? (-100 .. +100), rP = 1 ?
      parameter Km = 1 ?, kcat = 0.1 ?, So = 10
[output]
   directory ./project/NNMT/01/sub/Q/output/fit-P-local-R1
   rate-file ./project/NNMT/01/sub/Q/data/rates-local-R1.csv
   rate-scale 1000
[settings]
{Filter}
   XMin = 1
   XMax = 1200
{Output}
   XAxisLabel = t, sec
   YAxisLabel = {/Symbol D}F/10^6, rfu
[end]
;_____________________________________________________________________________
;_____________________________________________________________________________
```

A.3. Determination of the apparent Michaelis constant for quinoline

The following DynaFit script file was used to fit initial reaction rates to determine the apparent Michaelis constant for quinoline. The reaction rates exported automatically the DynaFit script listed in Appendix A.2 were pooled into a single data file.

```
;_____________________________________________________________________________
[task]
   task = fit
   data = rates
   approximation = rapid-equilibrium
[mechanism]
   E + S <==> E.S          :    Km    dissoc
   E.S ---> E + P          :    kcat
[constants]
   Km = 10 ??
   kcat = 0.1 ??
[concentrations]
   E = 0.1
[responses]
   P = 1
[data]
   variable S
   directory ./project/NNMT/01/sub/Q/data
graph quinoline K_m :: from local fit to Lambert Omega function
```

```
   sheet rates-local-R123.csv
   column 2
[output]
   directory ./project/NNMT/01/sub/Q/output/fit-V-local-R123
[settings]
{Filter}
   AverageReplicates = y
{Output}
   XAxisLabel = [Quinoline], {/Symbol m}M
   YAxisLabel = v/10^3, rfu/sec
   PredictionBands = y
[end]
;_____________________________________________________________________________
;_____________________________________________________________________________
```

A.4. Global fit of inhibition data, Cpd **31**, *Rep 1*

The following DynaFit script file was used to fit one of the three replicates (in this case R1) of inhibition data involving compound **31** to the three candidate mechanisms displayed in section 4.2, which are represented mathematically by the ODE systems shown in Appendix B.2.

```
Fixed 'kcat', 3 models
;_____________________________________________________________________________
[task]
   task = fit
   data = progress
   model = R1S ?
[mechanism]
   E + S <==> E.S       :     ka.S     kd.S
   E.S ---> E + P       :     kd.P
   E + P <==> E.P       :     ka.Pi    kd.Pi
   E + I <==> E.I       :     ka.I     kd.I
   E.S ---> F           :     k.ES
[constants]
   ka.S  = 10
   kd.S  = 11.8
   kd.P  = 0.036
   ka.Pi = 10
   kd.Pi = 2.06
   ka.I  = {0.00001, 0.0001, 0.001, 0.01, 0.1, 1, 10, 100} ??
   kd.I  = {0.00001, 0.0001, 0.001, 0.01, 0.1, 1, 10, 100, 1000, 10000} ??
   k.ES  = 0.00058
[concentrations]
   E = 0.1
   S = 10
[responses]
   P = 1 ?
[data]
   directory ./project/NNMT/01/inh/CPD-31/R1/data
   sheet CPD-31-R1.csv
   monitor E, E.S, E.I, F
```

```
graph (31) NS1-12'Me :: R1
 ; columns 1:2  | offset auto ?  | conc I =  31.6        | label  A1
 ; columns 3:4  | offset auto ?  | conc I =  10        | label  A2
 ; columns 5:6  | offset auto ?  | conc I =  3.16456        | label  A3
 ; columns 7:8  | offset auto ?  | conc I =  1.00144        | label  A4
   columns 9:10  | offset auto ?  | conc I =  0.316911        | label  A5
   columns 11:12  | offset auto ?  | conc I =  0.100288        | label  A6
   columns 13:14  | offset auto ?  | conc I =  0.0317367        | label  A7
   columns 15:16  | offset auto ?  | conc I =  0.0100433        | label  A8
   columns 17:18  | offset auto ?  | conc I =  0.00317826        | label  A9
   columns 19:20  | offset auto ?  | conc I =  0.00100578        | label  A10
   columns 21:22  | offset auto ?  | conc I =  0        | label  A11
   columns 23:24  | offset auto ?  | conc I =  0        | label  A12

[output]
   directory ./project/NNMT/01/inh/CPD-31/R1/output/fit-CPD-31-R1-001
[settings]
{Filter}
   XMin = 0
   XMax = 1200
   ZeroBaselineSignal = y
{Output}
   XAxisLabel = t, sec
   YAxisLabel = {/Symbol D}F, rfu
   WriteTeX = y
{Constraints}
   Concentrations = 1.414
{ConfidenceIntervals}
   SquaresIncreasePercent = 1
   OnlyConstants = n
{EstimateScan}
   RefineEstimates = 30
{ModelSelection}
   OnlyConstants = y
   CoefficientOfVariationMax = 1000000000000
   CoefficientOfVariationSearchMax = 1000000000000
;_____________________________________________________________________
[task]
   task = fit
   data = progress
   model = R1F ?
[mechanism]
   E + S <==> E.S       :     ka.S     kd.S
   E.S ---> E + P       :     kd.P
   E + P <==> E.P       :     ka.Pi    kd.Pi
   E + I <==> E.I       :     ka.I     kd.I
   E.S ---> F           :     k.ES
[constants]
   ka.S  = 10
   kd.S  = 11.8
   kd.P  = 0.036
```

```
   ka.Pi = 10
   kd.Pi = 2.06
   ka.I  = 10
   kd.I  = {0.00001, 0.0001, 0.001, 0.01, 0.1, 1, 10, 100, 1000, 10000} ??
   k.ES  = 0.00058
;_____________________________________________________________________________
[task]
   task = fit
   data = progress
   model = C1 ?
[mechanism]
   E + S <==> E.S       :     ka.S     kd.S
   E.S ---> E + P       :     kd.P
   E + P <==> E.P       :     ka.Pi    kd.Pi
   E + I ---> E.I       :     ka.I
   E.S ---> F           :     k.ES
[constants]
   ka.S  = 10
   kd.S  = 11.8
   kd.P  = 0.036
   ka.Pi = 10
   kd.Pi = 2.06
   ka.I  = {0.00001, 0.0001, 0.001, 0.01, 0.1, 1, 10, 100} ??
   k.ES  = 0.00058
[end]
;_____________________________________________________________________________
;_____________________________________________________________________________
```

The DynaFit script listed above corresponds to **Method A**, where the "k_{cat}" rate constant labeled $k_{d.I}$ is treated as a fixed parameter set to the value determined independently as described in section 1.3.2.

A nearly identical DynaFit script was utilized to analyze the same data according to **Method B**, where the the "k_{cat}" rate constant labeled $k_{d.I}$ is treated as an optimized model parameter. The only difference between the two methods is the following line in the input script:

Method A

```
[constants]
...
   kd.P  = 0.036
...
```

Method B

```
[constants]
...
   kd.P  = 0.036 ?
...
```

Note that appending a question mark to the numerical value of any item listed in the DynaFit input script will transform it from a fixed constant to an adjustable or tunable model parameter.

B. Systems of ODEs automatically derived by DynaFit

This appendix contains systems of first-order ordinary differential equations (ODEs) automatically derived by the software package DynaFit [4] from symbolic input files listed in Appendix A.

B.1. Substrate kinetics of SAM

B.1.1. Model **MM**

The following system first-order ordinary differential equations describes the time course of an enzyme reaction following the simple Michaelis-Menten mechanism.

See section 1.2.1 for a symbolic representation.

$$\frac{\mathrm{d}[\mathrm{E}]}{\mathrm{d}t} = -k_{\mathrm{a.S}}[\mathrm{E}][\mathrm{S}] + k_{\mathrm{d.S}}[\mathrm{E.S}] + k_{\mathrm{d.P}}[\mathrm{E.S}] \tag{S16}$$

$$\frac{\mathrm{d}[\mathrm{S}]}{\mathrm{d}t} = -k_{\mathrm{a.S}}[\mathrm{E}][\mathrm{S}] + k_{\mathrm{d.S}}[\mathrm{E.S}] \tag{S17}$$

$$\frac{\mathrm{d}[\mathrm{E.S}]}{\mathrm{d}t} = +k_{\mathrm{a.S}}[\mathrm{E}][\mathrm{S}] - k_{\mathrm{d.S}}[\mathrm{E.S}] - k_{\mathrm{d.P}}[\mathrm{E.S}] \tag{S18}$$

$$\frac{\mathrm{d}[\mathrm{P}]}{\mathrm{d}t} = +k_{\mathrm{d.P}}[\mathrm{E.S}] \tag{S19}$$

B.1.2. Model **MM+pi**

The following system first-order ordinary differential equations describes the time course of an enzyme reaction following the Michaelis-Menten mechanism accompanied by product inhibition.

See section 1.2.2 for a symbolic representation.

$$\frac{\mathrm{d}[\mathrm{E}]}{\mathrm{d}t} = -k_{\mathrm{a.S}}[\mathrm{E}][\mathrm{S}] + k_{\mathrm{d.S}}[\mathrm{E.S}] + k_{\mathrm{d.P}}[\mathrm{E.S}] - k_{\mathrm{a.Pi}}[\mathrm{E}][\mathrm{P}] + k_{\mathrm{d.Pi}}[\mathrm{E.P}] \tag{S20}$$

$$\frac{\mathrm{d}[\mathrm{S}]}{\mathrm{d}t} = -k_{\mathrm{a.S}}[\mathrm{E}][\mathrm{S}] + k_{\mathrm{d.S}}[\mathrm{E.S}] \tag{S21}$$

$$\frac{\mathrm{d}[\mathrm{E.S}]}{\mathrm{d}t} = +k_{\mathrm{a.S}}[\mathrm{E}][\mathrm{S}] - k_{\mathrm{d.S}}[\mathrm{E.S}] - k_{\mathrm{d.P}}[\mathrm{E.S}] \tag{S22}$$

$$\frac{\mathrm{d}[\mathrm{P}]}{\mathrm{d}t} = +k_{\mathrm{d.P}}[\mathrm{E.S}] - k_{\mathrm{a.Pi}}[\mathrm{E}][\mathrm{P}] + k_{\mathrm{d.Pi}}[\mathrm{E.P}] \tag{S23}$$

$$\frac{\mathrm{d}[\mathrm{E.P}]}{\mathrm{d}t} = +k_{\mathrm{a.Pi}}[\mathrm{E}][\mathrm{P}] - k_{\mathrm{d.Pi}}[\mathrm{E.P}] \tag{S24}$$

B.1.3. Model **MM+ed**

The following system first-order ordinary differential equations describes the time course of an enzyme reaction following the Michaelis-Menten mechanism accompanied by enzyme deactivation via fist-order decay of the Michaelis complex ES.

See section 1.2.3 for a symbolic representation.

$$\frac{\mathrm{d}[\mathrm{E}]}{\mathrm{d}t} = -k_{\mathrm{a.S}}[\mathrm{E}][\mathrm{S}] + k_{\mathrm{d.S}}[\mathrm{E.S}] + k_{\mathrm{d.P}}[\mathrm{E.S}] \tag{S25}$$

$$\frac{\mathrm{d}[\mathrm{S}]}{\mathrm{d}t} = -k_{\mathrm{a.S}}[\mathrm{E}][\mathrm{S}] + k_{\mathrm{d.S}}[\mathrm{E.S}] \tag{S26}$$

$$\frac{\mathrm{d}[\mathrm{E.S}]}{\mathrm{d}t} = +k_{\mathrm{a.S}}[\mathrm{E}][\mathrm{S}] - k_{\mathrm{d.S}}[\mathrm{E.S}] - k_{\mathrm{d.P}}[\mathrm{E.S}] - k_{\mathrm{.ES}}[\mathrm{E.S}] \tag{S27}$$

$$\frac{\mathrm{d}[\mathrm{P}]}{\mathrm{d}t} = +k_{\mathrm{d.P}}[\mathrm{E.S}] \tag{S28}$$

$$\frac{\mathrm{d}[\mathrm{F}]}{\mathrm{d}t} = +k_{\mathrm{.ES}}[\mathrm{E.S}] \tag{S29}$$

B.1.4. Model **MM+pi+ed**

The following system first-order ordinary differential equations describes the time course of an enzyme reaction following the Michaelis-Menten mechanism accompanied by (a) product inhibition and (b) enzyme deactivation via fist-order decay of the Michaelis complex ES.

See section 1.2.4 for a symbolic representation.

$$\frac{\mathrm{d}[\mathrm{E}]}{\mathrm{d}t} = -k_{\mathrm{a.S}}[\mathrm{E}][\mathrm{S}] + k_{\mathrm{d.S}}[\mathrm{E.S}] + k_{\mathrm{d.P}}[\mathrm{E.S}] - k_{\mathrm{a.Pi}}[\mathrm{E}][\mathrm{P}] + k_{\mathrm{d.Pi}}[\mathrm{E.P}] \tag{S30}$$

$$\frac{\mathrm{d}[\mathrm{S}]}{\mathrm{d}t} = -k_{\mathrm{a.S}}[\mathrm{E}][\mathrm{S}] + k_{\mathrm{d.S}}[\mathrm{E.S}] \tag{S31}$$

$$\frac{\mathrm{d}[\mathrm{E.S}]}{\mathrm{d}t} = +k_{\mathrm{a.S}}[\mathrm{E}][\mathrm{S}] - k_{\mathrm{d.S}}[\mathrm{E.S}] - k_{\mathrm{d.P}}[\mathrm{E.S}] - k_{\mathrm{.ES}}[\mathrm{E.S}] \tag{S32}$$

$$\frac{\mathrm{d}[\mathrm{P}]}{\mathrm{d}t} = +k_{\mathrm{d.P}}[\mathrm{E.S}] - k_{\mathrm{a.Pi}}[\mathrm{E}][\mathrm{P}] + k_{\mathrm{d.Pi}}[\mathrm{E.P}] \tag{S33}$$

$$\frac{\mathrm{d}[\mathrm{E.P}]}{\mathrm{d}t} = +k_{\mathrm{a.Pi}}[\mathrm{E}][\mathrm{P}] - k_{\mathrm{d.Pi}}[\mathrm{E.P}] \tag{S34}$$

$$\frac{\mathrm{d}[\mathrm{F}]}{\mathrm{d}t} = +k_{\mathrm{.ES}}[\mathrm{E.S}] \tag{S35}$$

B.2. Inhibition kinetics

B.2.1. Models **R1S** *and* **R1F**

The following system first-order ordinary differential equations describes the time course of an enzyme reaction following the Michaelis-Menten mechanism accompanied by (a) product inhibition and (b) enzyme deactivation via fist-order decay of the Michaelis complex ES.

In addition, the inhibitor I binds to the enzyme E in a competitive manner (i.e., with mutual exclusion) with respect to the substrate S. Inhibitor binding is assumed to be reversible.

See section 4.2.2 for a symbolic representation of the mechanism.

$$\begin{aligned}
\frac{\mathrm{d}[\mathrm{E}]}{\mathrm{d}t} &= -k_{\mathrm{a.S}}[\mathrm{E}][\mathrm{S}] + k_{\mathrm{d.S}}[\mathrm{E.S}] + k_{\mathrm{d.P}}[\mathrm{E.S}] - k_{\mathrm{a.Pi}}[\mathrm{E}][\mathrm{P}] + k_{\mathrm{d.Pi}}[\mathrm{E.P}] && \text{(S36)}\\
&\quad -k_{\mathrm{a.I}}[\mathrm{E}][\mathrm{I}] + k_{\mathrm{d.I}}[\mathrm{E.I}] \\
\frac{\mathrm{d}[\mathrm{S}]}{\mathrm{d}t} &= -k_{\mathrm{a.S}}[\mathrm{E}][\mathrm{S}] + k_{\mathrm{d.S}}[\mathrm{E.S}] && \text{(S37)}\\
\frac{\mathrm{d}[\mathrm{E.S}]}{\mathrm{d}t} &= +k_{\mathrm{a.S}}[\mathrm{E}][\mathrm{S}] - k_{\mathrm{d.S}}[\mathrm{E.S}] - k_{\mathrm{d.P}}[\mathrm{E.S}] - k_{\mathrm{.ES}}[\mathrm{E.S}] && \text{(S38)}\\
\frac{\mathrm{d}[\mathrm{P}]}{\mathrm{d}t} &= +k_{\mathrm{d.P}}[\mathrm{E.S}] - k_{\mathrm{a.Pi}}[\mathrm{E}][\mathrm{P}] + k_{\mathrm{d.Pi}}[\mathrm{E.P}] && \text{(S39)}\\
\frac{\mathrm{d}[\mathrm{E.P}]}{\mathrm{d}t} &= +k_{\mathrm{a.Pi}}[\mathrm{E}][\mathrm{P}] - k_{\mathrm{d.Pi}}[\mathrm{E.P}] && \text{(S40)}\\
\frac{\mathrm{d}[\mathrm{F}]}{\mathrm{d}t} &= +k_{\mathrm{.ES}}[\mathrm{E.S}] && \text{(S41)}\\
\frac{\mathrm{d}[\mathrm{I}]}{\mathrm{d}t} &= -k_{\mathrm{a.I}}[\mathrm{E}][\mathrm{I}] + k_{\mathrm{d.I}}[\mathrm{E.I}] && \text{(S42)}\\
\frac{\mathrm{d}[\mathrm{E.I}]}{\mathrm{d}t} &= +k_{\mathrm{a.I}}[\mathrm{E}][\mathrm{I}] - k_{\mathrm{d.I}}[\mathrm{E.I}] && \text{(S43)}
\end{aligned}$$

B.2.2. Model **C1**

The following system first-order ordinary differential equations describes the time course of an enzyme reaction following the Michaelis-Menten mechanism accompanied by (a) product inhibition and (b) enzyme deactivation via fist-order decay of the Michaelis complex ES.

In addition, the inhibitor I binds to the enzyme E in a competitive manner (i.e., with mutual exclusion) with respect to the substrate S. Inhibitor binding is assumed to be nominally irreversible.

In the physical as opposed to purely formal and mathematical domain, "irreversible" binding means that either the inhibitor is binding covalently *or* that the inhibitor is binding reversibly but, at the same time, the dissociation rate constant $k_{\mathrm{d.I}}$ is so extremely low that the lower limit of its confidence interval, at the given confidence level, cannot be reliably determined from the given set of experimental data.

See section 4.2.4 for a symbolic representation of the mechanism.

$$\frac{\mathrm{d}[\mathrm{E}]}{\mathrm{d}t} = -k_{\mathrm{a.S}}[\mathrm{E}][\mathrm{S}] + k_{\mathrm{d.S}}[\mathrm{E.S}] + k_{\mathrm{d.P}}[\mathrm{E.S}] - k_{\mathrm{a.Pi}}[\mathrm{E}][\mathrm{P}] + k_{\mathrm{d.Pi}}[\mathrm{E.P}] \quad \text{(S44)}$$

$$-k_{\mathrm{a.I}}[\mathrm{E}][\mathrm{I}]$$

$$\frac{\mathrm{d}[\mathrm{S}]}{\mathrm{d}t} = -k_{\mathrm{a.S}}[\mathrm{E}][\mathrm{S}] + k_{\mathrm{d.S}}[\mathrm{E.S}] \quad \text{(S45)}$$

$$\frac{\mathrm{d}[\mathrm{E.S}]}{\mathrm{d}t} = +k_{\mathrm{a.S}}[\mathrm{E}][\mathrm{S}] - k_{\mathrm{d.S}}[\mathrm{E.S}] - k_{\mathrm{d.P}}[\mathrm{E.S}] - k_{\mathrm{.ES}}[\mathrm{E.S}] \quad \text{(S46)}$$

$$\frac{\mathrm{d}[\mathrm{P}]}{\mathrm{d}t} = +k_{\mathrm{d.P}}[\mathrm{E.S}] - k_{\mathrm{a.Pi}}[\mathrm{E}][\mathrm{P}] + k_{\mathrm{d.Pi}}[\mathrm{E.P}] \quad \text{(S47)}$$

$$\frac{\mathrm{d}[\mathrm{E.P}]}{\mathrm{d}t} = +k_{\mathrm{a.Pi}}[\mathrm{E}][\mathrm{P}] - k_{\mathrm{d.Pi}}[\mathrm{E.P}] \quad \text{(S48)}$$

$$\frac{\mathrm{d}[\mathrm{F}]}{\mathrm{d}t} = +k_{\mathrm{.ES}}[\mathrm{E.S}] \quad \text{(S49)}$$

$$\frac{\mathrm{d}[\mathrm{I}]}{\mathrm{d}t} = -k_{\mathrm{a.I}}[\mathrm{E}][\mathrm{I}] \quad \text{(S50)}$$

$$\frac{\mathrm{d}[\mathrm{E.I}]}{\mathrm{d}t} = +k_{\mathrm{a.I}}[\mathrm{E}][\mathrm{I}] \quad \text{(S51)}$$

C. Model-selection results

This appendix contains model-selection results automatically derived by the software package DynaFit [4] from symbolic input files listed in Appendix A.

In the auto-generated tables below, the meaning of mathematical symbols that appear in the table headings is as follows:

Value	best-fit value of the given model parameter
StdErr	formal standard error of each parameter computed from diagonal elements of the covariance matrix
CV %	coefficient of variation
Low	lower limit of the confidence interval
High	upper limit of the confidence interval
P(Low)	probability level reached at the lower bound of the confidence interval
P(High)	probability level reached at the upper bound of the confidence interval
n_{P}	number of adjustable model parameters
SSQ_{r}	relative sum of squared deviations
ΔAIC	differential Akaike Information Criterion
ΔBIC	differential Bayesian Information Criterion
$w^{(\mathrm{AIC})}$	Akaike weight
$w^{(\mathrm{BIC})}$	Bayesian weight

Model failures – Legend

:Delta ... Differential AIC/BIC criterion greater than 5
:Weight ... Akaike / Bayesian weight lower than 0.01
:Squares ... Relative sum of squared deviations greater than 1.05

For further details regarding the mathematical and statistical principles of model discrimination implemented in the DynaFit software pacakge,, see refs. [4, 11–13].

C.1. Substrate kinetics of SAM

C.1.1. Replicate R1

Intermediate results

Kinetic constants

Model	Parameter	Value	StdErr	CV %	Low	High	P(Low) %	P(High) %
MM	kd.S	21.3	2.1	19.1	18	25.3	96.3	96.3
	kd.P	0.0348	0.0028	15.5	0.029	0.04	96.3	96.3
MM+Pi	kd.S	0.0588	0.0045	14.3	0.05	0.0691	96.3	96.3
	kd.P	0.0108	0.0017	29.5	0.00926	0.0125	96.3	96.3
	kd.Pi	0.00366	0.00065	33.0	0.00304	0.00448	96.3	96.3
MM+Ed	kd.S	44.4	2.8	11.9	39.8	49.8	96.3	96.3
	kd.P	0.0523	0.0026	9.3	0.0468	0.0575	96.3	96.3
	k.ES	0.00128	5.1e-005	7.4	0.00119	0.00138	96.3	96.3
MM+Pi+Ed	kd.S	8	1	22.4	6.07	10	96.2	96.2
	kd.P	0.0301	0.00086	5.1	0.0283	0.0319	96.2	96.2
	kd.Pi	0.984	0.15	27.8	0.701	1.32	96.2	96.2
	k.ES	0.000678	2.3e-005	6.2	0.00063	0.000727	96.2	96.2

Information-Theoretic Criteria – Full Set

model	n_P	SSQ_r	ΔAIC	ΔBIC	$w^{(AIC)}$	$w^{(BIC)}$	parameters
MM+Pi+Ed	15	1.000	0.0	0.0	1.000	1.000	OK
MM+Pi	14	2.796	460.5	456.3	0.000	0.000	OK
MM+Ed	14	6.099	811.5	807.4	0.000	0.000	OK
MM	13	24.770	1440.0	1431.8	0.000	0.000	OK

Final results

Information-Theoretic Criteria – Reduced Set

model	n_P	SSQ_r	ΔAIC	ΔBIC	$w^{(AIC)}$	$w^{(BIC)}$	status
MM+Pi+Ed	15	1.000	0.0	0.0	1.000	1.000	OK
MM+Pi	14	2.796	460.5	456.3	0.000	0.000	FAIL:Squares
MM+Ed	14	6.099	811.5	807.4	0.000	0.000	FAIL:Squares
MM	13	24.770	1440.0	1431.8	0.000	0.000	FAIL:Squares

Model Discrimination Analysis – Conclusions

A single candidate model passes all acceptance criteria:

task no.	model ID	n_P	SSQ_r	Δ AIC	Δ BIC
4	MM+Pi+Ed	15	1	0	0

Acceptable parameters

Model	Parameter	Value	Low	High
MM+Pi+Ed	kd.S	8	6.07	10
	kd.P	0.0301	0.0283	0.0319
	kd.Pi	0.984	0.701	1.32
	k.ES	0.000678	0.00063	0.000727

C.1.2. Replicate R2

Intermediate results

Kinetic constants

Model	Parameter	Value	StdErr	CV %	Low	High	P(Low) %	P(High) %
MM	kd.S	22.9	1.9	16.1	19.7	26.5	96.3	96.3
	kd.P	0.0398	0.0024	11.6	0.0348	0.0444	96.3	96.3
MM+Pi	kd.S	0.0636	0.0069	20.1	0.0512	0.0819	96.3	96.3
	kd.P	0.0192	0.001	9.9	0.0169	0.0214	96.3	96.3
	kd.Pi	0.00789	0.00091	21.6	0.00618	0.0104	96.3	96.3
MM+Ed	kd.S	44.4	2.3	9.7	40.5	48.9	96.3	96.3
	kd.P	0.0562	0.0021	6.9	0.0518	0.0604	96.3	96.3
	k.ES	0.0011	3.9e-005	6.7	0.00103	0.00118	96.3	96.3
MM+Pi+Ed	kd.S	12.8	0.94	13.2	10.9	14.8	96.2	96.2
	kd.P	0.0376	0.00079	3.8	0.036	0.0393	96.2	96.2
	kd.Pi	2.69	0.28	18.5	2.15	3.3	96.2	96.2
	k.ES	0.000542	2.1e-005	7.0	0.000499	0.000586	96.2	96.2

Information-Theoretic Criteria – Full Set

model	n_P	SSQ_r	ΔAIC	ΔBIC	$w^{(AIC)}$	$w^{(BIC)}$	parameters
MM+Pi+Ed	15	1.000	0.0	0.0	1.000	1.000	OK
MM+Pi	14	2.316	375.8	371.7	0.000	0.000	OK
MM+Ed	14	5.265	745.3	741.2	0.000	0.000	OK
MM	13	22.847	1403.7	1395.5	0.000	0.000	OK

Final results

Information-Theoretic Criteria – Reduced Set

model	n_P	SSQ_r	ΔAIC	ΔBIC	$w^{(AIC)}$	$w^{(BIC)}$	status
MM+Pi+Ed	15	1.000	0.0	0.0	1.000	1.000	OK
MM+Pi	14	2.316	375.8	371.7	0.000	0.000	FAIL:Squares
MM+Ed	14	5.265	745.3	741.2	0.000	0.000	FAIL:Squares
MM	13	22.847	1403.7	1395.5	0.000	0.000	FAIL:Squares

Model Discrimination Analysis – Conclusions

A single candidate model passes all acceptance criteria:

task no.	model ID	n_P	SSQ_r	Δ AIC	Δ BIC
4	MM+Pi+Ed	15	1	0	0

Acceptable parameters

Model	Parameter	Value	Low	High
MM+Pi+Ed	kd.S	12.8	10.9	14.8
	kd.P	0.0376	0.036	0.0393
	kd.Pi	2.69	2.15	3.3
	k.ES	0.000542	0.000499	0.000586

C.1.3. Replicate R3

Intermediate results

Kinetic constants

Model	Parameter	Value	StdErr	CV %	Low	High	P(Low) %	P(High) %
MM	kd.S	24.8	2.1	16.3	21.5	28.7	96.3	96.3
	kd.P	0.043	0.0025	11.4	0.0376	0.0479	96.3	96.3
MM+Pi	kd.S	0.0991	0.016	30.9	0.0681	0.19	96.3	96.3
	kd.P	0.0239	0.001	8.1	0.0213	0.0267	96.3	96.3
	kd.Pi	0.013	0.002	28.9	0.00896	0.0241	96.3	96.3
MM+Ed	kd.S	48.9	2.6	9.8	44.5	53.7	96.3	96.3
	kd.P	0.0611	0.0022	6.8	0.0565	0.0656	96.3	96.3
	k.ES	0.00113	4.1e-005	6.8	0.00105	0.00121	96.3	96.3
MM+Pi+Ed	kd.S	15.8	1	11.5	13.8	17.9	96.2	96.2
	kd.P	0.0411	0.00084	3.7	0.0393	0.0428	96.2	96.2
	kd.Pi	3.29	0.31	16.7	2.7	3.96	96.2	96.2
	k.ES	0.000543	2.2e-005	7.2	0.000498	0.000588	96.2	96.2

Information-Theoretic Criteria – Full Set

model	n_P	SSQ_r	ΔAIC	ΔBIC	$w^{(AIC)}$	$w^{(BIC)}$	parameters
MM+Pi+Ed	15	1.000	0.0	0.0	1.000	1.000	OK
MM+Pi	14	2.415	394.6	390.5	0.000	0.000	OK
MM+Ed	14	5.415	758.0	753.9	0.000	0.000	OK
MM	13	24.028	1426.4	1418.1	0.000	0.000	OK

Final results

Information-Theoretic Criteria – Reduced Set

model	n_P	SSQ_r	ΔAIC	ΔBIC	$w^{(AIC)}$	$w^{(BIC)}$	status
MM+Pi+Ed	15	1.000	0.0	0.0	1.000	1.000	OK
MM+Pi	14	2.415	394.6	390.5	0.000	0.000	FAIL:Squares
MM+Ed	14	5.415	758.0	753.9	0.000	0.000	FAIL:Squares
MM	13	24.028	1426.4	1418.1	0.000	0.000	FAIL:Squares

Model Discrimination Analysis – Conclusions

A single candidate model passes all acceptance criteria:

task no.	model ID	n_P	SSQ_r	Δ AIC	Δ BIC
4	MM+Pi+Ed	15	1	0	0

Acceptable parameters

Model	Parameter	Value	Low	High
MM+Pi+Ed	kd.S	15.8	13.8	17.9
	kd.P	0.0411	0.0393	0.0428
	kd.Pi	3.29	2.7	3.96
	k.ES	0.000543	0.000498	0.000588

C.2. Inhibitor kinetics of compound **18**

Intermediate results

Kinetic constants

Model	Parameter	Value	StdErr	CV %	Low	High	P(Low) %	P(High) %
R1S	ka.I	5.35e+006	3.1e+008	5906.1	0.0837	1.68e+008	74.2	0
	kd.I	1.8e+007	1e+009	5908.3	0.28	2e+006	74.2	0
R1F	kd.I	33.5	2	6.4	31.4	35.8	74.4	74.4
C1	ka.I	0.00116	8.2e-005	7.4	0.00107	0.00126	74.4	74.4

Information-Theoretic Criteria – Full Set

model	n_P	SSQ_r	ΔAIC	ΔBIC	$w^{(AIC)}$	$w^{(BIC)}$	parameters
R1F	13	1.000	0.0	0.0	0.776	0.938	OK
R1S	14	1.000	2.5	5.4	0.224	0.062	FAIL:UB
C1	13	1.885	90.6	90.6	0.000	0.000	OK

Parameter failures – Legend

:LB ... Missing lower bound for at least one parameter
:UB ... Missing upper bound
:UB/LB ... Upper-to-lower bound ratio too large
:CV ... Coefficient of variation too large

Final results

Information-Theoretic Criteria – Reduced Set

model	n_P	SSQ_r	ΔAIC	ΔBIC	$w^{(AIC)}$	$w^{(BIC)}$	status
R1F	13	1.000	0.0	0.0	1.000	1.000	OK
C1	13	1.884	90.6	90.6	0.000	0.000	FAIL:Squares

Model failures – Legend
:Delta ... Differential AIC/BIC criterion greater than 5
:Weight ... Akaike / Bayesian weight lower than 0.01
:Squares ... Relative sum of squared deviations greater than 1.05

Model Discrimination Analysis – Conclusions

A single candidate model passes all acceptance criteria:

task no.	model ID	n_P	SSQ_r	Δ AIC	Δ BIC
2	R1F	13	1.00008	0	0

Acceptable parameters

Model	Parameter	Value	Low	High
R1F	kd.I	33.5	31.4	35.8

C.3. Inhibitor kinetics of compound **26**

Intermediate results

Kinetic constants

Model	Parameter	Value	StdErr	CV %	Low	High	P(Low) %	P(High) %
R1S	ka.I	0.365	0.0096	5.0	0.347	0.383	93.7	93.7
	kd.I	0.000134	3.8e-005	53.0	6.39e-005	0.000207	93.7	93.7
R1F	kd.I	0.0235	0.00096	8.0	0.0218	0.0254	93.8	93.8
C1	ka.I	0.335	0.0038	2.2	0.328	0.342	93.8	93.8

Information-Theoretic Criteria – Full Set

model	n_P	SSQ_r	ΔAIC	ΔBIC	$w^{(AIC)}$	$w^{(BIC)}$	parameters
R1S	11	1.000	0.0	0.0	0.996	0.973	OK
C1	10	1.037	11.1	7.2	0.004	0.027	OK
R1F	10	7.475	722.0	718.1	0.000	0.000	OK

Final results

Information-Theoretic Criteria – Reduced Set

model	n_P	SSQ_r	ΔAIC	ΔBIC	$w^{(AIC)}$	$w^{(BIC)}$	status
R1S	11	1.000	0.0	0.0	0.996	0.973	OK
C1	10	1.037	11.1	7.2	0.004	0.027	OK
R1F	10	7.475	722.0	718.1	0.000	0.000	FAIL:Squares

Model failures – Legend
:Delta ... Differential AIC/BIC criterion greater than 5
:Weight ... Akaike / Bayesian weight lower than 0.01
:Squares ... Relative sum of squared deviations greater than 1.05

Model Discrimination Analysis – Conclusions

2 Different candidate models pass all acceptance criteria:

task no.	model ID	n_P	SSQ_r	Δ AIC	Δ BIC
1	R1S	11	1	0	0
3	C1	10	1.03742	11.0862	7.20007

Acceptable parameters

Model	Parameter	Value	Low	High
R1S	ka.I	0.365	0.347	0.383
	kd.I	0.000134	6.39e-005	0.000207
C1	ka.I	0.335	0.328	0.342

C.4. Inhibitor kinetics of compound **31**

C.4.1. Replicate 1

Intermediate results

Kinetic constants

Model	Parameter	Value	StdErr	CV %	Low	High	P(Low) %	P(High) %
R1S	ka.I	4.96	3.4	68.8	2.75	16.4	66.3	66.3
	kd.I	0.0168	0.012	73.2	0.00871	0.0575	66.3	66.3
R1F	kd.I	0.0348	0.0033	9.6	0.0317	0.038	66.5	66.5
C1	ka.I	0.818	0.063	7.9	0.755	0.887	66.5	66.5

Information-Theoretic Criteria – Full Set

model	n_P	SSQ_r	ΔAIC	ΔBIC	$w^{(AIC)}$	$w^{(BIC)}$	parameters
R1F	10	1.005	0.0	0.0	0.735	0.912	OK
R1S	11	1.000	2.0	4.7	0.265	0.088	OK
C1	10	1.355	31.1	31.1	0.000	0.000	OK

Final results

Information-Theoretic Criteria – Reduced Set

model	n_P	SSQ_r	ΔAIC	ΔBIC	$w^{(AIC)}$	$w^{(BIC)}$	status
R1F	10	1.005	0.0	0.0	0.735	0.912	OK
R1S	11	1.000	2.0	4.7	0.265	0.088	OK
C1	10	1.355	31.1	31.1	0.000	0.000	FAIL:Squares

Model failures – Legend

:Delta ... Differential AIC/BIC criterion greater than 5

:Weight ... Akaike / Bayesian weight lower than 0.01

:Squares ... Relative sum of squared deviations greater than 1.05

Model Discrimination Analysis – Conclusions

2 Different candidate models pass all acceptance criteria:

task no.	model ID	n_P	SSQ_r	Δ AIC	Δ BIC
1	R1S	11	1	2.03538	4.67977
2	R1F	10	1.00505	0	0

Acceptable parameters

Model	Parameter	Value	Low	High
R1S	ka.I	4.96	2.75	16.4
	kd.I	0.0168	0.00871	0.0575
R1F	kd.I	0.0348	0.0317	0.038

C.4.2. Replicate 2

Intermediate results

Kinetic constants

Model	Parameter	Value	StdErr	CV %	Low	High	P(Low) %	P(High) %
R1S	ka.I	2.57	0.96	37.4	1.85	4	66.3	66.3
	kd.I	0.00968	0.0043	44.2	0.00644	0.0158	66.3	66.3
R1F	kd.I	0.0407	0.0034	8.7	0.0374	0.0443	66.5	66.5
C1	ka.I	0.707	0.05	7.2	0.656	0.764	66.5	66.5

Information-Theoretic Criteria – Full Set

model	n_P	SSQ_r	ΔAIC	ΔBIC	$w^{(AIC)}$	$w^{(BIC)}$	parameters
R1S	11	1.000	0.0	0.1	0.779	0.485	OK
R1F	10	1.050	2.5	0.0	0.221	0.515	OK
C1	10	1.423	34.1	31.6	0.000	0.000	OK

Final results

Information-Theoretic Criteria – Reduced Set

model	n_P	SSQ_r	ΔAIC	ΔBIC	$w^{(AIC)}$	$w^{(BIC)}$	status
R1S	11	1.000	0.0	0.1	0.779	0.485	OK
R1F	10	1.050	2.5	0.0	0.221	0.515	FAIL:Squares
C1	10	1.423	34.1	31.6	0.000	0.000	FAIL:Squares

Model failures – Legend

:Delta ... Differential AIC/BIC criterion greater than 5
:Weight ... Akaike / Bayesian weight lower than 0.01
:Squares ... Relative sum of squared deviations greater than 1.05

Model Discrimination Analysis – Conclusions

A single candidate model passes all acceptance criteria:

task no.	model ID	n_P	SSQ_r	Δ AIC	Δ BIC
1	R1S	11	1	0	0.123159

Acceptable parameters

Model	Parameter	Value	Low	High
R1S	ka.I	2.57	1.85	4
	kd.I	0.00968	0.00644	0.0158

C.4.3. Replicate 3

Intermediate results

Kinetic constants

Model	Parameter	Value	StdErr	CV %	Low	High	P(Low) %	P(High) %
R1S	ka.I	3.41	1.2	35.7	2.5	5.24	66.3	66.3
	kd.I	0.00845	0.0036	42.6	0.0057	0.0137	66.3	66.3
R1F	kd.I	0.0268	0.0023	8.9	0.0247	0.0291	66.5	66.5
C1	ka.I	0.994	0.07	7.2	0.925	1.07	66.5	66.5

Information-Theoretic Criteria – Full Set

model	n_P	SSQ_r	ΔAIC	ΔBIC	$w^{(AIC)}$	$w^{(BIC)}$	parameters
R1S	11	1.000	0.0	1.4	0.653	0.334	OK
R1F	10	1.037	1.3	0.0	0.347	0.666	OK
C1	10	1.414	33.5	32.2	0.000	0.000	OK

Final results

Information-Theoretic Criteria – Reduced Set

model	n_P	SSQ_r	ΔAIC	ΔBIC	$w^{(AIC)}$	$w^{(BIC)}$	status
R1S	11	1.000	0.0	1.4	0.653	0.334	OK
R1F	10	1.037	1.3	0.0	0.347	0.666	OK
C1	10	1.414	33.5	32.2	0.000	0.000	FAIL:Squares

Model failures – Legend

:Delta ... Differential AIC/BIC criterion greater than 5
:Weight ... Akaike / Bayesian weight lower than 0.01
:Squares ... Relative sum of squared deviations greater than 1.05

Model Discrimination Analysis – Conclusions

2 Different candidate models pass all acceptance criteria:

task no.	model ID	n_P	SSQ_r	Δ AIC	Δ BIC
1	R1S	11	1	0	1.37715
2	R1F	10	1.03748	1.26724	0

Acceptable parameters

Model	Parameter	Value	Low	High
R1S	ka.I	3.41	2.5	5.24
	kd.I	0.00845	0.0057	0.0137
R1F	kd.I	0.0268	0.0247	0.0291